

# TMDPDFs extractions with DNNs

*Ishara Fernando & Dustin Keller*

2025 EIC User Group Early Career Workshop

*July 11-13, 2025  
Jefferson Lab  
Newport News, VA, US.*

Based on : <https://doi.org/10.1103/PhysRevD.108.054007>



UNIVERSITY  
of VIRGINIA



U.S. DEPARTMENT OF  
**ENERGY**

Office of  
Science

This work is supported by DOE contract DE-FG02-96ER40950

# Outline

- Motivation
- A brief introduction to TMDs
- Sivers asymmetry from SIDIS
- DNN Approach for  $SU(3)_{\text{flavor}}$
- DNN Method Testing
- DNN Fits & Results for Sivers function
- Unpolarized TMDs extraction
- Summary and Outlook

# Motivation

- TMDs: so far, model-dependent extractions  $\rightarrow$  assumptions, limitations and biases
- Information from data: Has the full potential of the data been taken into account?

Introducing this ‘novel’ method of extracting TMDs with Deep Neural Networks (DNNs)  
First time in TMD extractions (published in 2023)

- Capacity to handle complex patterns, relationships in data with multi-D dependence.
- Data-driven
- Minimally biased  $\rightarrow$  un-biased
- Uncertainty propagation (from data) using bootstrap method by generating ‘replicas’  
(Statistical & Systematic uncertainties from the experimental data are combined in quadrature)
- Recursive improvements to the DNN
- Systematic component can be quantified by a dedicated analysis

Intended to be  
Exploratory & Instructional

# TMDPDFs

$$\Phi(x, k_T; S) = \int \frac{d\xi^- d\xi_T}{(2\pi)^3} e^{ik \cdot \xi} \langle P, S | \bar{\psi}(0) \mathcal{U}_{[0, \xi]} \psi(\xi) | P, S \rangle |_{\xi^+ = 0}$$

At leading-twist, the Quark correlator can be decomposed into 8 components (6 T - even and 2 T -odd terms)

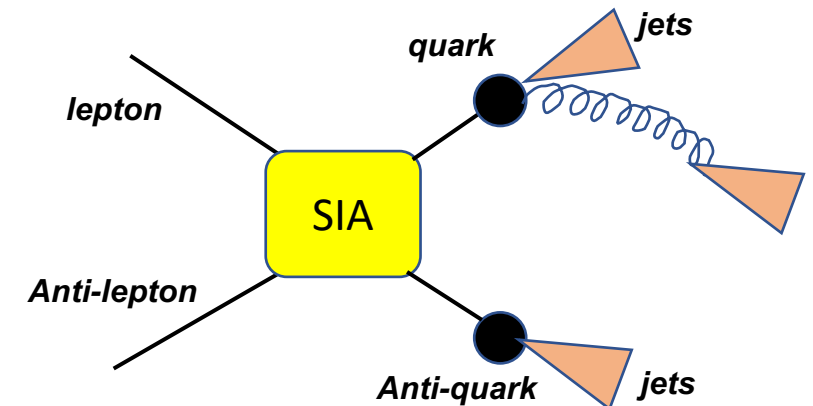
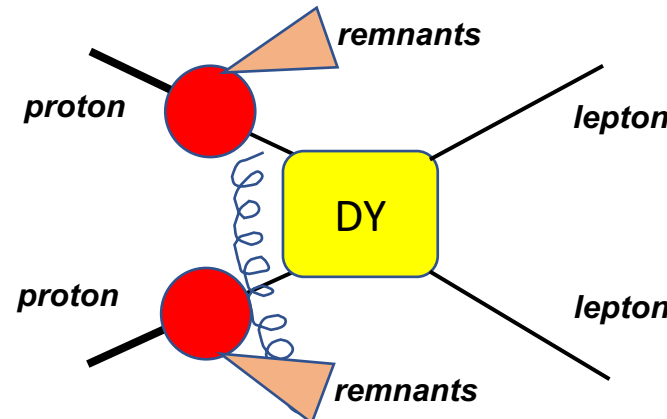
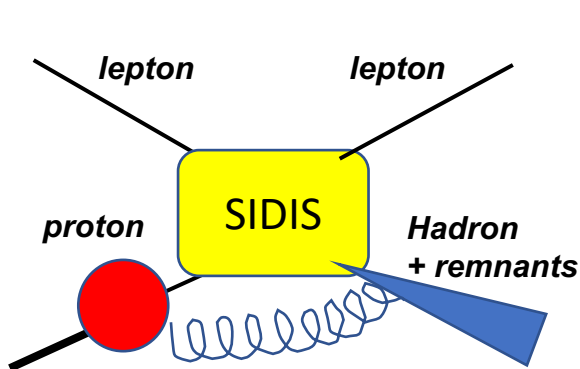
Leading Twist	Quark Polarization		
	Unpolarized [U]	Circular [L]	Linear [T]
Target Polarization	U $f_1$ Unpolarized		$h_1^\perp$ Boer-Mulders
	L	$g_1$ Helicity	$h_{1L}^\perp$ Worm-gear 1
	T $f_{1T}^\perp$ Sivers	$g_{1T}$ Worm-gear 2	$h_1$ Transversity $h_{1T}^\perp$ Pretzelosity
	TENSOR $\theta_{LL}(x, \mathbf{k}_T^2)$ $\theta_{TT}(x, \mathbf{k}_T^2)$ $\theta_{LT}(x, \mathbf{k}_T^2)$	$g_{1TT}(x, \mathbf{k}_T^2)$ $g_{1LT}(x, \mathbf{k}_T^2)$	$h_{1LL}^\perp(x, \mathbf{k}_T^2)$ $h_{1TT}(x, \mathbf{k}_T^2), h_{1TT}^\perp(x, \mathbf{k}_T^2)$ $h_{1LT}(x, \mathbf{k}_T^2), h_{1LT}^\perp(x, \mathbf{k}_T^2)$

$$\begin{aligned} \Phi(x, k_T, P, S) = & f_1(x, k_T^2) \frac{\not{P}}{2} + \frac{h_{1T}(x, k_T^2)}{4} \gamma_5 [\not{S}_T, \not{P}] + \frac{S_L}{2} g_{1L}(x, k_T^2) \gamma_5 \not{P} + \frac{k_T \cdot S_T}{2M} g_{1T}(x, k_T^2) \gamma_5 \not{P} \\ & + S_L h_{1L}^\perp(x, k_T^2) \gamma_5 \frac{[k_T, \not{P}]}{4M} + \frac{k_T \cdot S_T}{2M} h_{1T}^\perp(x, k_T^2) \gamma_5 \frac{[k_T, \not{P}]}{4M} \end{aligned}$$

T-even

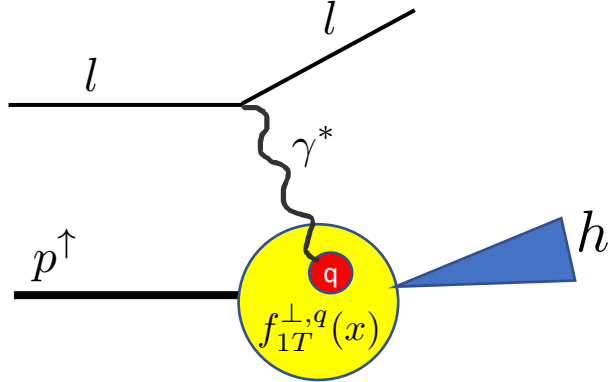
$$+ i h_1^\perp(x, k_T^2) \frac{[k_T, \not{P}]}{4M} - \frac{\epsilon_T^{k_T S_T}}{4M} f_{1T}^\perp(x, k_T^2) \not{P}$$

T-odd



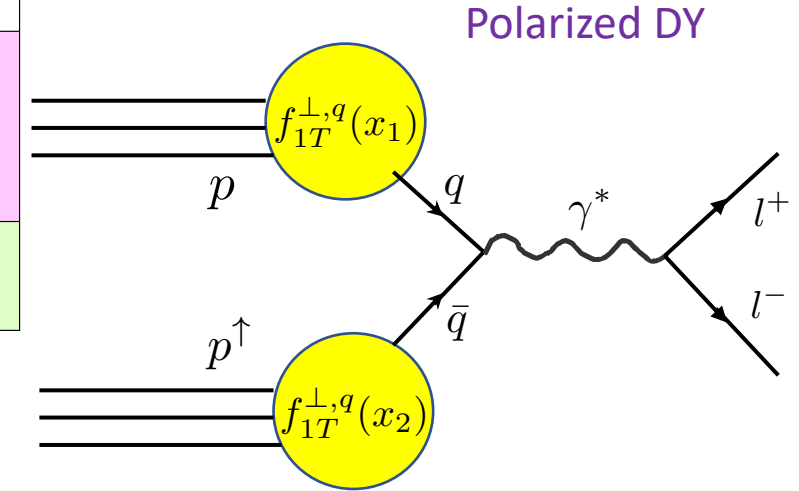
# TMDPDFs

## Polarized Semi Inclusive DIS



Leading Twist	Quark Polarization		
	Unpolarized [U]	Circular [L]	Linear [T]
Target Polarization	U $f_1$ Unpolarized		$h_1^\perp$ Boer-Mulders
	L $g_1$	Helicity	$h_{1L}^\perp$ Worm-gear 1
	T $f_{1T}^\perp$ Sivers	$g_{1T}$ Worm-gear 2	$h_1$ Transversity $h_{1T}^\perp$ Pretzelosity
	TENSOR $\theta_{LL}(x, \mathbf{k}_T^2)$ $\theta_{TT}(x, \mathbf{k}_T^2)$ $\theta_{LT}(x, \mathbf{k}_T^2)$	$g_{1TT}(x, \mathbf{k}_T^2)$ $g_{1LT}(x, \mathbf{k}_T^2)$	$h_{1LL}^\perp(x, \mathbf{k}_T^2)$ $h_{1TT}(x, \mathbf{k}_T^2), h_{1T}^\perp(x, \mathbf{k}_T^2)$ $h_{1LT}(x, \mathbf{k}_T^2), h_{1T}^\perp(x, \mathbf{k}_T^2)$

\* For these two processes  
TMD factorization is proven



$$\frac{d\sigma_{SIDIS}^{LO}}{dx dy dz dp_T^2 d\phi_h d\psi} = \left[ \frac{\alpha}{xyQ^2} \frac{y^2}{2(1-\epsilon)} \left( 1 + \frac{y^2}{2x} \right) \right] \times (F_{UU,T} + \epsilon F_{UU,L}) \left\{ 1 + \cos 2\phi_h \left( \epsilon A_{UU}^{\cos 2\phi_h} \right) + S_T \left[ \sin(\phi_h - \phi_s) \left( A_{UT}^{\sin(\phi_h - \phi_s)} \right) + \sin(\phi_h + \phi_s) \left( \epsilon A_{UT}^{\sin(\phi_h + \phi_s)} \right) + \sin(3\phi_h - \phi_s) \left( \epsilon A_{UT}^{\sin(3\phi_h - \phi_s)} \right) \right] \right\}$$

$$\frac{d\sigma^{LO}}{d\Omega} = \frac{\alpha_{em}^2}{F_q} F_v^1 \left\{ 1 + \cos^2 \theta + \sin^2 \theta \cos 2\phi_{CS} A_U^{\cos 2\phi_{CS}} + S_T \left[ (1 + \cos^2 \theta) \sin \phi_s A_T^{\sin \phi_s} + \sin^2 \theta \left( \sin(2\phi_{CS} + \phi_s) A_T^{\sin(2\phi_{CS} + \phi_s)} + \sin(2\phi_{CS} - \phi_s) A_T^{\sin(2\phi_{CS} - \phi_s)} \right) \right] \right\}$$

$$\begin{aligned} A_{UU}^{\cos 2\phi_h} &\propto h_1^{\perp q} \otimes H_{1q}^{\perp h} & \text{BM} \otimes \text{CF} \\ A_{UT}^{\sin(\phi_h - \phi_s)} &\propto f_{1T}^{\perp q} \otimes D_{1q}^h & \text{Sivers} \otimes \text{FF} \\ A_{UT}^{\sin(\phi_h + \phi_s)} &\propto h_1^q \otimes H_{1q}^{\perp h} & \text{Transv} \otimes \text{CF} \\ A_{UT}^{\sin(3\phi_h - \phi_s)} &\propto h_{1T}^{\perp q} \otimes H_{1q}^{\perp h} & \text{Pretz} \otimes \text{CF} \end{aligned}$$

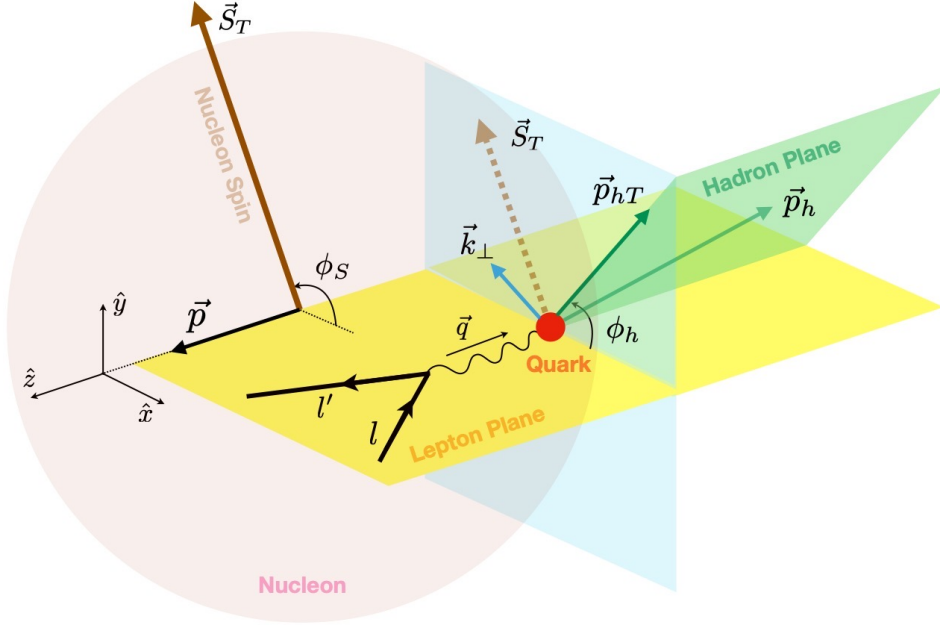
$$\begin{aligned} h_1^{\perp q} \Big|_{SIDIS} &= -h_1^{\perp q} \Big|_{DY} \\ f_{1T}^{\perp q} \Big|_{SIDIS} &= -f_{1T}^{\perp q} \Big|_{DY} \end{aligned}$$

$$\begin{aligned} h_1^q \Big|_{SIDIS} &= h_1^q \Big|_{DY} \\ h_{1T}^{\perp q} \Big|_{SIDIS} &= h_{1T}^{\perp q} \Big|_{DY} \end{aligned}$$

$$\begin{aligned} A_T^{\cos 2\phi_{CS}} &\propto h_1^{\perp q} \otimes h_1^{\perp q} & \text{BM} \otimes \text{BM} \\ A_T^{\sin \phi_s} &\propto f_1^q \otimes f_{1T}^{\perp q} & \text{PDF} \otimes \text{Sivers} \\ A_T^{\sin(2\phi_{CS} - \phi_s)} &\propto h_1^{\perp q} \otimes h_1^q & \text{BM} \otimes \text{Transv} \\ A_T^{\sin(2\phi_{CS} + \phi_s)} &\propto h_1^{\perp q} \otimes h_{1T}^{\perp q} & \text{BM} \otimes \text{Pretz} \end{aligned}$$

# Sivers Asymmetry from SIDIS

$$\frac{d^5\sigma^{lp\rightarrow lhX}}{dx dQ^2 dz d^2p_\perp} = \sum_q e_q^2 \int d^2\mathbf{k}_\perp \left( \frac{2\pi\alpha^2}{x^2 s^2} \frac{\hat{s}^2 + \hat{u}^2}{Q^4} \right) \times \hat{f}_{q/p^\uparrow}(x, k_\perp) D_{h/q}(z, p_\perp) + \mathcal{O}(k_\perp/Q) ,$$



$$\hat{f}_{q/p^\uparrow}(x, k_\perp) = f_{q/p}(x, k_\perp) + \frac{1}{2} \Delta^N f_{q/p^\uparrow}(x, k_\perp) \vec{S}_T \cdot (\hat{p} \times \hat{k}_\perp)$$

$$\Delta^N f_{q/p^\uparrow}(x, k_\perp) = 2\mathcal{N}_q(x) h(k_\perp) f_{q/p}(x, k_\perp)$$

Anselmino et al. (2017)

## Single Spin Asymmetry (Sivers Asymmetry)

$$A_{UT}^{\sin(\phi_h - \phi_S)}(x, y, z, p_{hT}) = \frac{d\sigma^{l^\uparrow p \rightarrow hlX} - d\sigma^{l^\downarrow p \rightarrow hlX}}{d\sigma^{l^\uparrow p \rightarrow hlX} + d\sigma^{l^\downarrow p \rightarrow hlX}} \equiv \frac{d\sigma^\uparrow - d\sigma^\downarrow}{d\sigma^\uparrow + d\sigma^\downarrow}$$

$$\langle p_\perp^2 \rangle = 0.12 \pm 0.01 \text{ GeV}^2$$

$$\langle k_\perp^2 \rangle = 0.57 \pm 0.08 \text{ GeV}^2$$

$$\begin{aligned} \mathcal{A}_0(z, p_{hT}, m_1) &= \frac{\sqrt{2} e z p_{hT}}{m_1} \frac{[z^2 \langle k_\perp^2 \rangle + \langle p_\perp^2 \rangle] \langle k_S^2 \rangle^2}{[z^2 \langle k_S^2 \rangle + \langle p_\perp^2 \rangle]^2 \langle k_\perp^2 \rangle} \\ &\times \exp \left[ - \frac{p_{hT}^2 z^2 (\langle k_S^2 \rangle - \langle k_\perp^2 \rangle)}{(z^2 \langle k_S^2 \rangle + \langle p_\perp^2 \rangle) (z^2 \langle k_\perp^2 \rangle + \langle p_\perp^2 \rangle)} \right] \\ \langle k_S^2 \rangle &= \frac{m_1 \langle k_\perp^2 \rangle}{m_1^2 + \langle k_\perp^2 \rangle} \end{aligned}$$

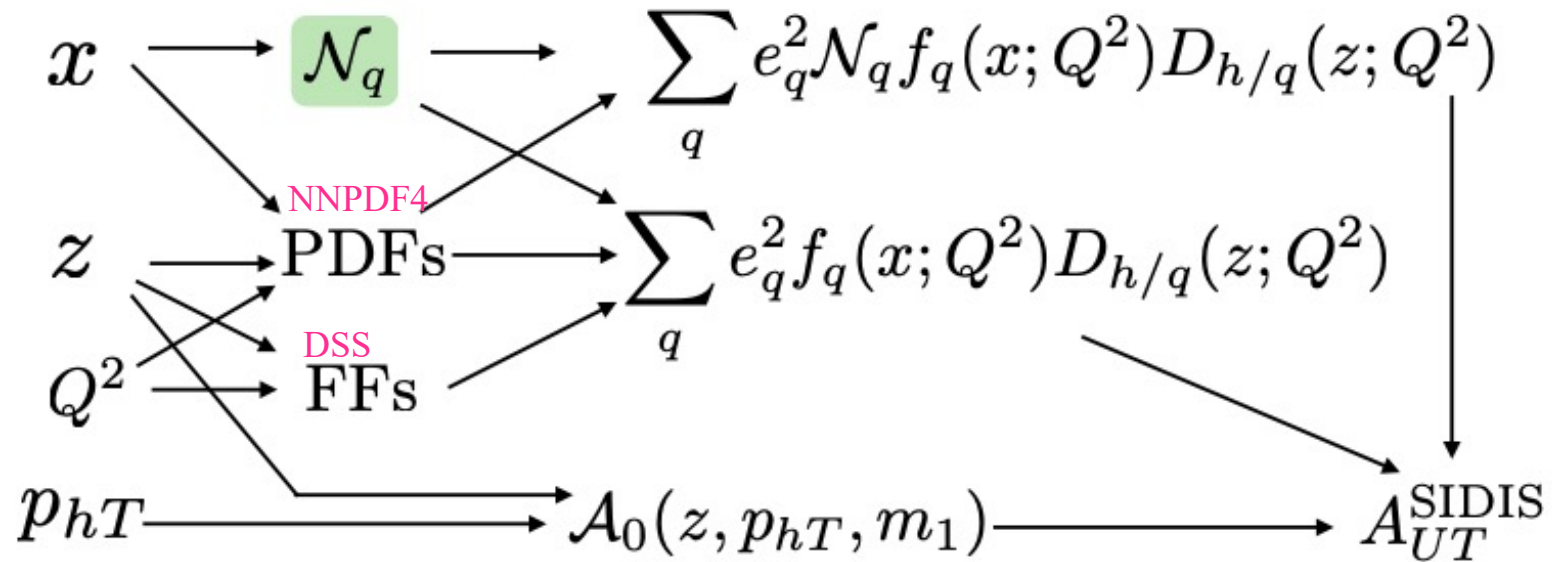
$$A_{UT}^{\sin(\phi_h - \phi_S)}(x, z, p_{hT}) = \mathcal{A}_0(z, p_{hT}, m_1) \left( \frac{\sum_q \mathcal{N}_q(x) e_q^2 f_q(x) D_{h/q}(z)}{\sum_q e_q^2 f_q(x) D_{h/q}(z)} \right)$$

$$\mathcal{N}_q(x) = N_q x^{\alpha_q} (1-x)^{\beta_q} \frac{(\alpha_q + \beta_q)^{(\alpha_q + \beta_q)}}{\alpha_q^{\alpha_q} \beta_q^{\beta_q}}$$

$$\mathcal{N}_{\bar{q}}(x) = N_{\bar{q}}$$

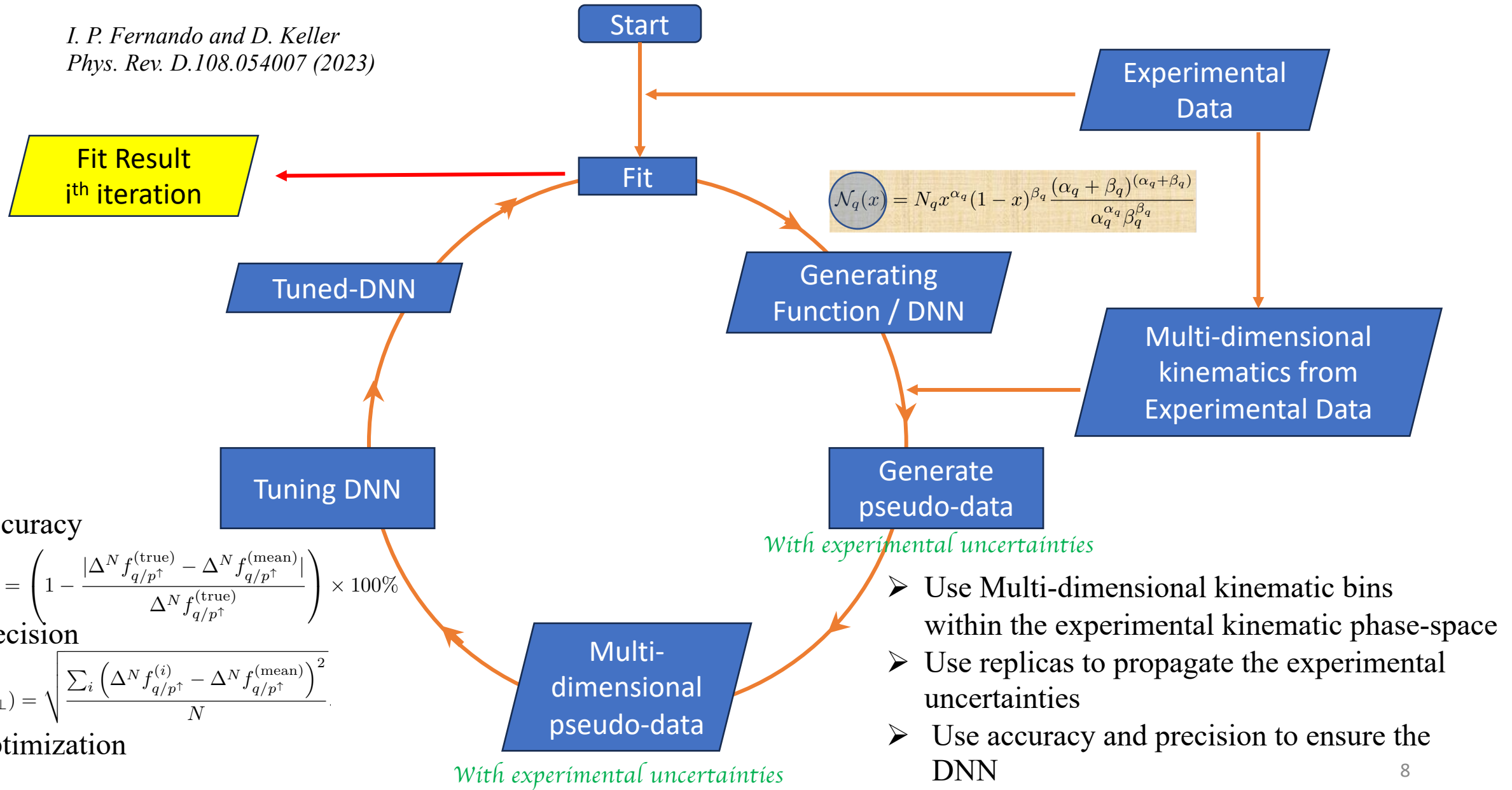
# DNN Approach

$$A_{UT}^{\sin(\phi_h - \phi_S)}(x, z, p_{hT}) = \mathcal{A}_0(z, p_{hT}, m_1) \left( \frac{\sum_q \mathcal{N}_q(x) e_q^2 f_q(x) D_{h/q}(z)}{\sum_q e_q^2 f_q(x) D_{h/q}(z)} \right)$$

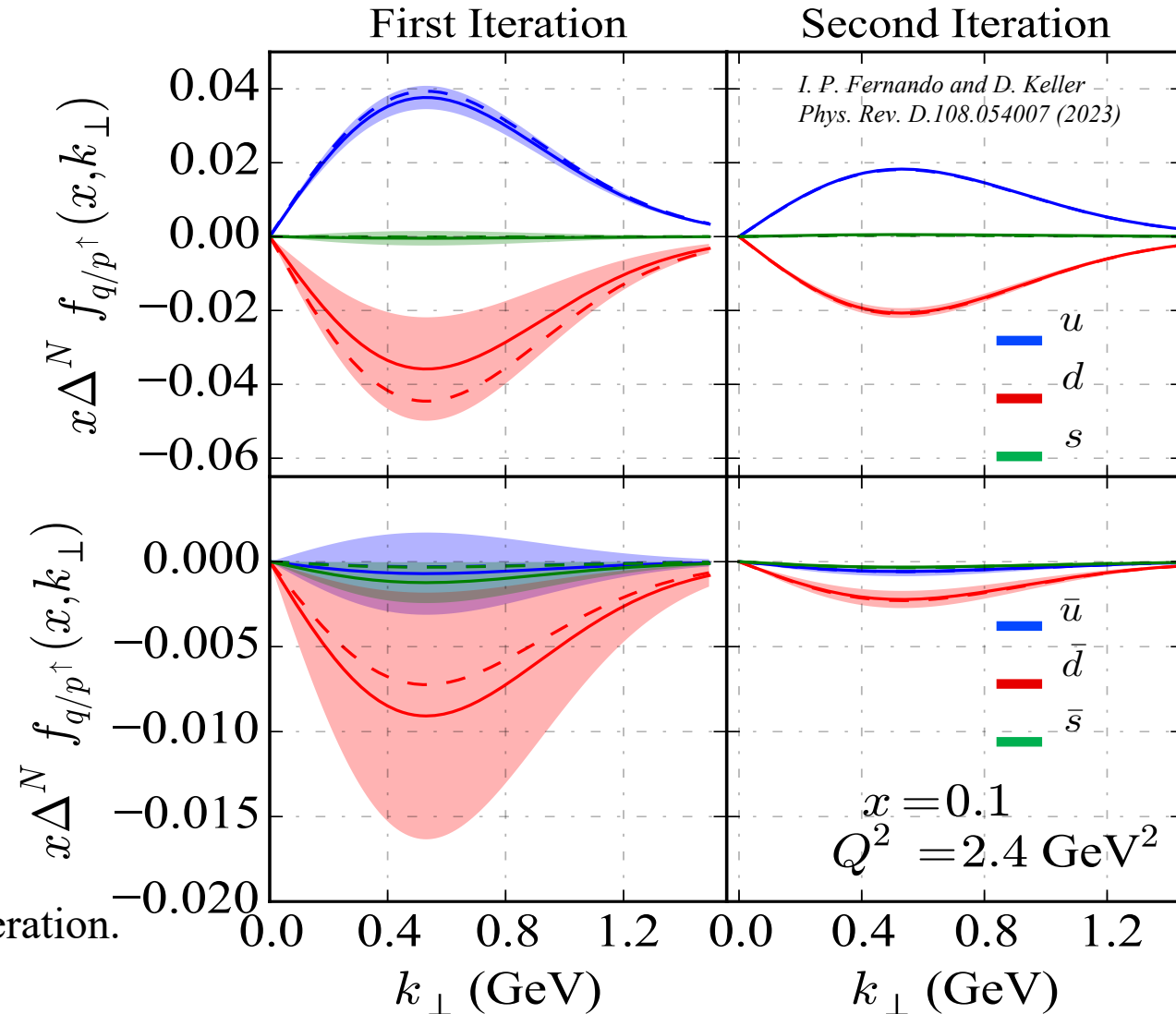
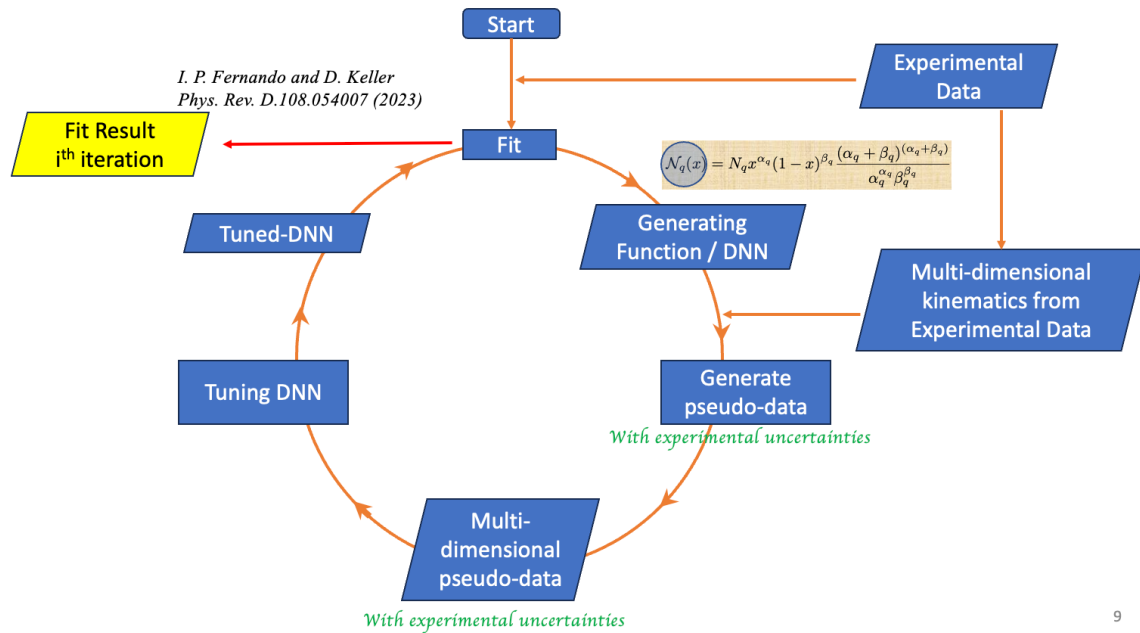


# The DNN Method for extracting Sivers function

*I. P. Fernando and D. Keller*  
*Phys. Rev. D.108.054007 (2023)*



# DNN Method testing



- Dashed lines represent the **generating function** in each iteration.
- A comparison: Improving the **generating function**  
Fine-tuning the hyperparameters
- Solid-lines and the band represent the mean and 68% CL with 1000 replicas of the DNN model.

# Data Selection

Proton DNN  
model

Deuteron DNN  
model

Projections from  
Deuteron DNN model

Dataset	Kinematic coverage	Reaction	Data points
HERMES2009 (SIDIS) [53]	$0.023 < x < 0.4$	$p^\uparrow + \gamma^* \rightarrow \pi^+$	21
	$0.2 < z < 0.7$	$p^\uparrow + \gamma^* \rightarrow \pi^-$	21
	$0.1 < p_{hT} < 0.9$	$p^\uparrow + \gamma^* \rightarrow \pi^0$	21
	$Q^2 > 1 \text{ GeV}^2$	$p^\uparrow + \gamma^* \rightarrow K^+$	21
		$p^\uparrow + \gamma^* \rightarrow K^-$	21
HERMES2020 (SIDIS) [55]	$0.023 < x < 0.6$	$p^\uparrow + \gamma^* \rightarrow \pi^+$	27, 64
	$0.2 < z < 0.7$	$p^\uparrow + \gamma^* \rightarrow \pi^-$	27, 64
	$0.1 < p_{hT} < 0.9$	$p^\uparrow + \gamma^* \rightarrow \pi^0$	27
	$Q^2 > 1 \text{ GeV}^2$	$p^\uparrow + \gamma^* \rightarrow K^+$	27, 64
		$p^\uparrow + \gamma^* \rightarrow K^-$	27, 64
COMPASS2015 (SIDIS) [54]	$0.006 < x < 0.28$	$p^\uparrow + \gamma^* \rightarrow \pi^+$	26
	$0.2 < z < 0.8$	$p^\uparrow + \gamma^* \rightarrow \pi^-$	26
	$0.15 < p_{hT} < 1.5$	$p^\uparrow + \gamma^* \rightarrow K^+$	26
	$Q^2 > 1 \text{ GeV}^2$	$p^\uparrow + \gamma^* \rightarrow K^-$	26
COMPASS2009 (SIDIS) [49]	$0.006 < x < 0.28$	$d^\uparrow + \gamma^* \rightarrow \pi^+$	26
	$0.2 < z < 0.8$	$d^\uparrow + \gamma^* \rightarrow \pi^-$	26
	$0.15 < p_{hT} < 1.5$	$d^\uparrow + \gamma^* \rightarrow K^+$	26
	$Q^2 > 1 \text{ GeV}^2$	$d^\uparrow + \gamma^* \rightarrow K^-$	26
JLAB2011 (SIDIS) [52]	$0.156 < x < 0.396$	$^3\text{He}^\uparrow + \gamma^* \rightarrow \pi^+$	4
	$0.50 < z < 0.58$	$^3\text{He}^\uparrow + \gamma^* \rightarrow \pi^-$	4
	$0.24 < p_{hT} < 0.43$ $1.3 < Q^2 < 2.7$		
COMPASS2017 (DY) [50]	$0.1 < x_N < 0.25$	$p^\uparrow + \pi^- \rightarrow l^+ l^- X$	15
	$0.3 < x_\pi < 0.7$		
	$4.3 < Q_M < 8.5$		
	$0.6 < q_T < 1.9$		

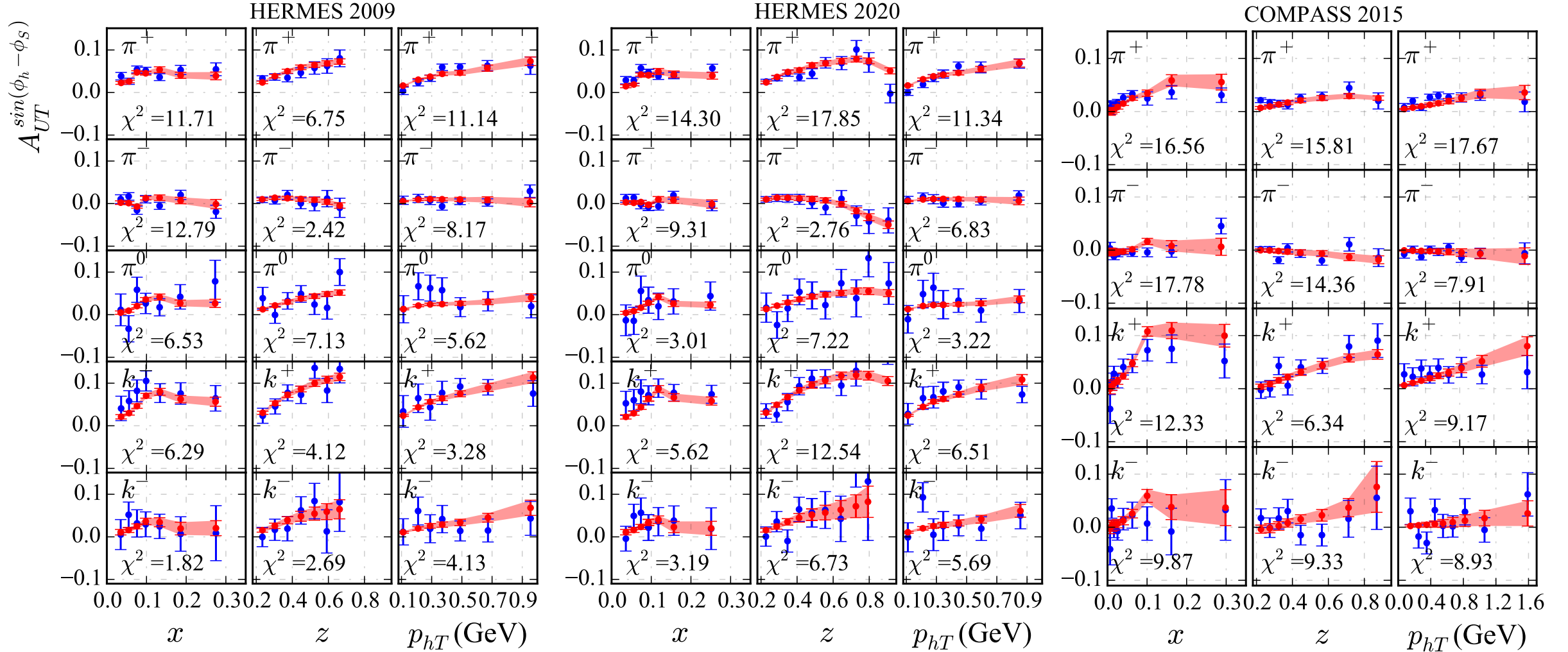
HERMES2020  
3D binned data

Projections from  
Proton DNN model

$$\Delta^N f_{q/p^\uparrow}(x, k_\perp)|_{\text{SIDIS}} = -\Delta^N f_{q/p^\uparrow}(x, k_\perp)|_{\text{DY}}$$

# Proton DNN Fit Results

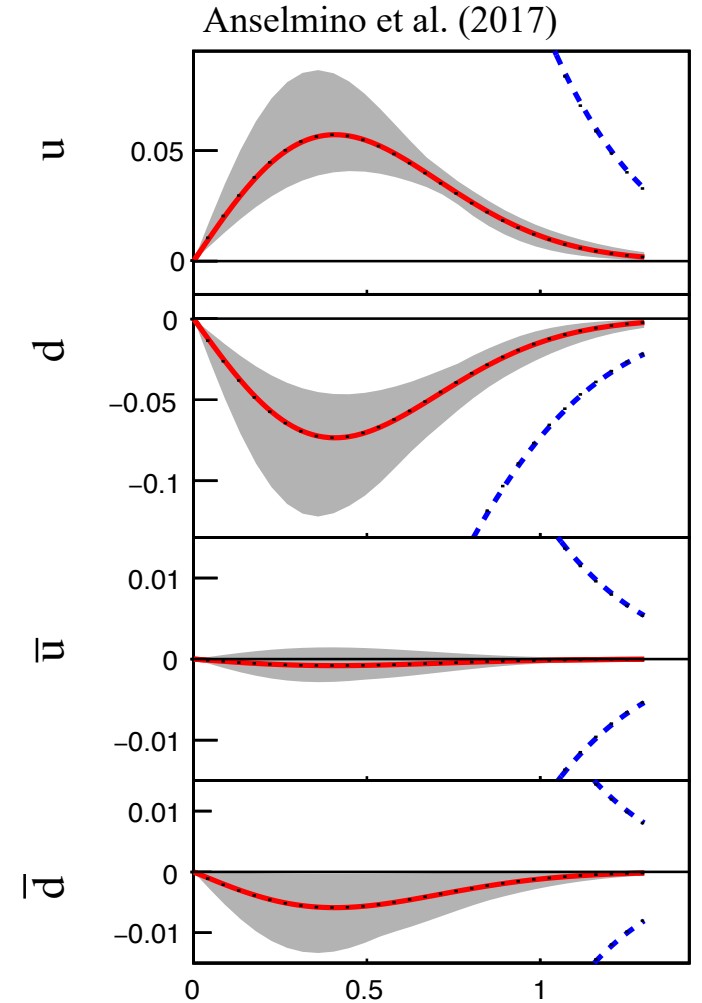
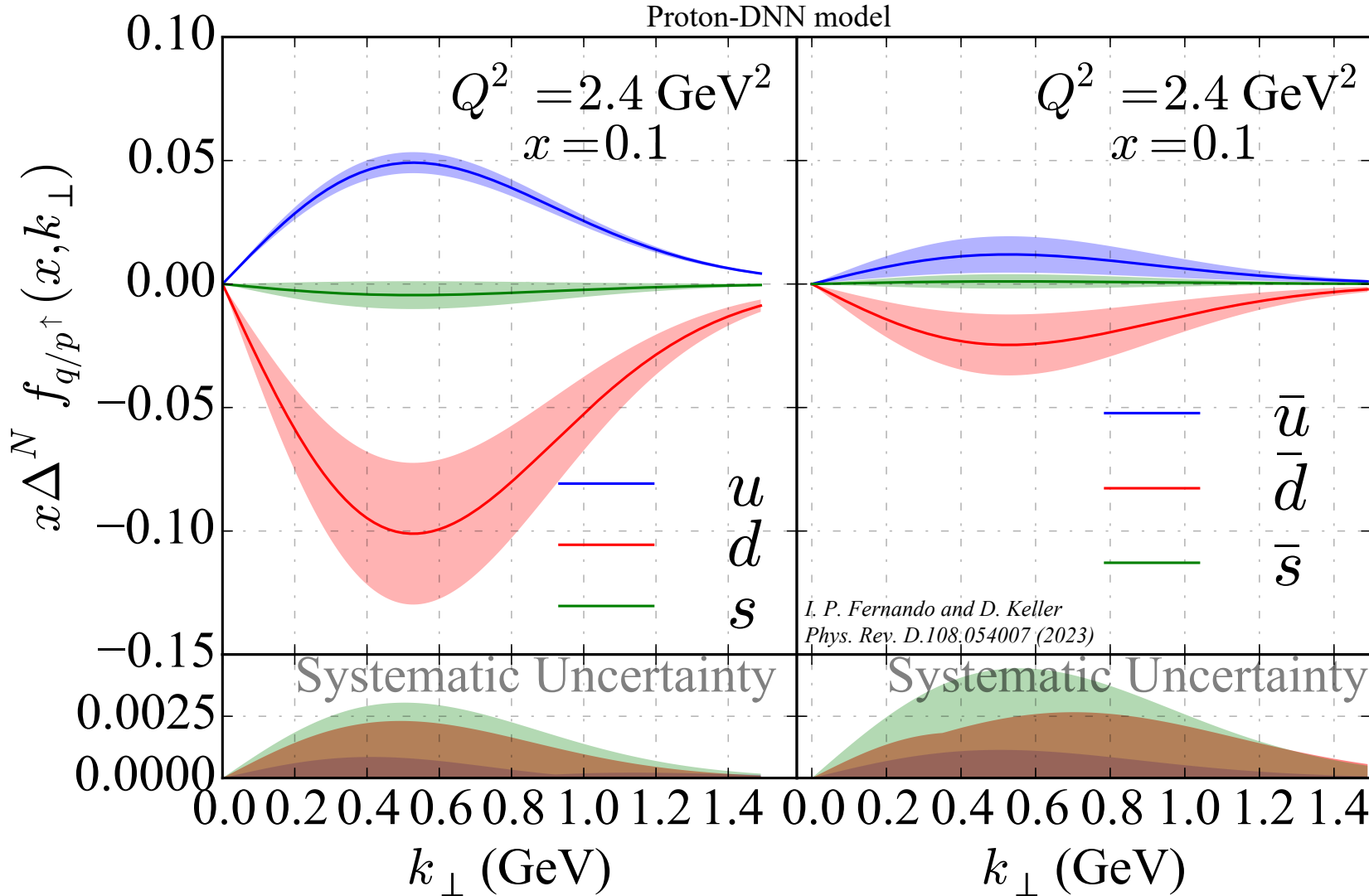
*I. P. Fernando and D. Keller  
Phys. Rev. D.108.054007 (2023)*



- All data points are well-described by the proton-DNN model.
- No kinematic cuts were implemented.

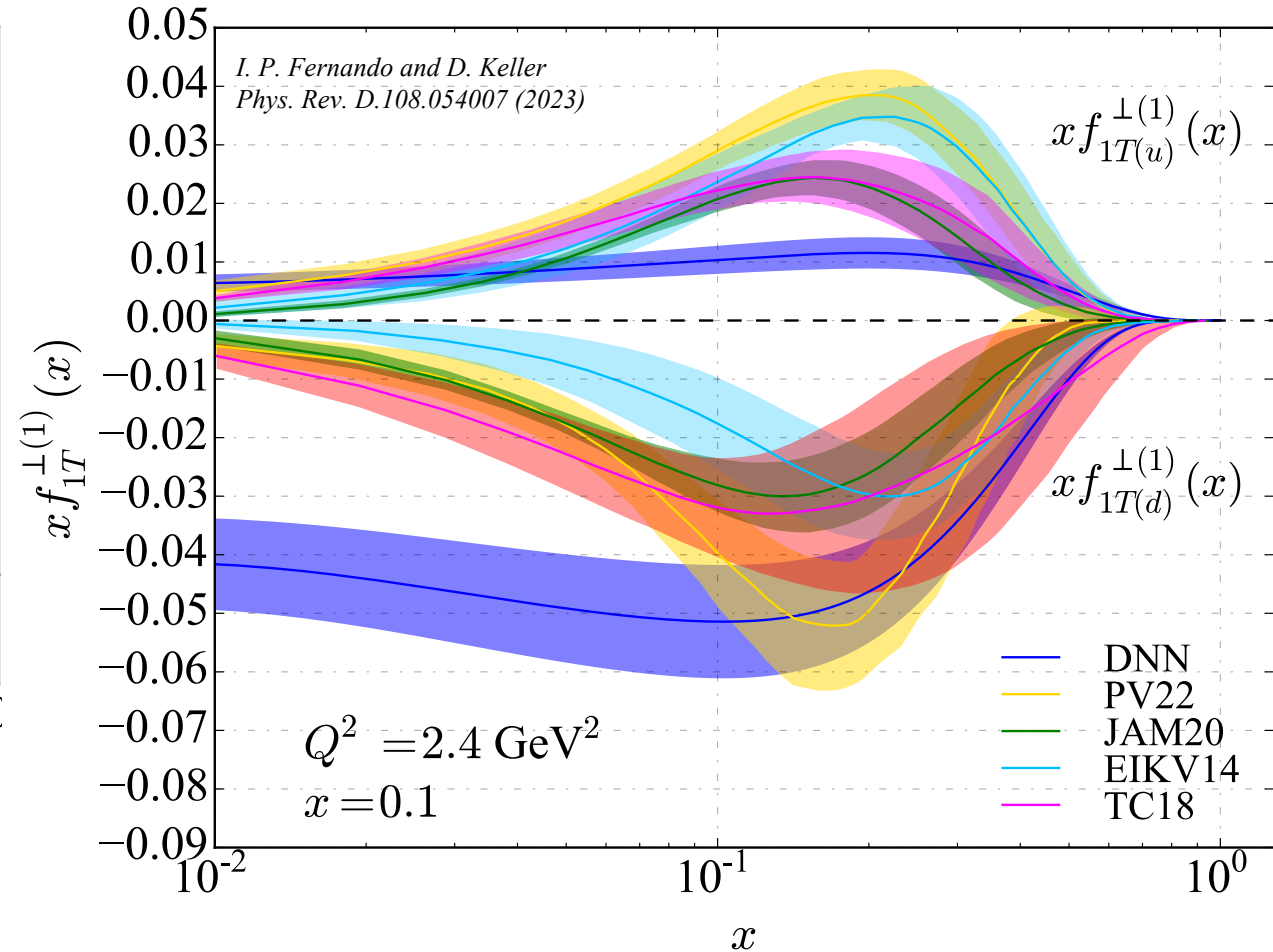
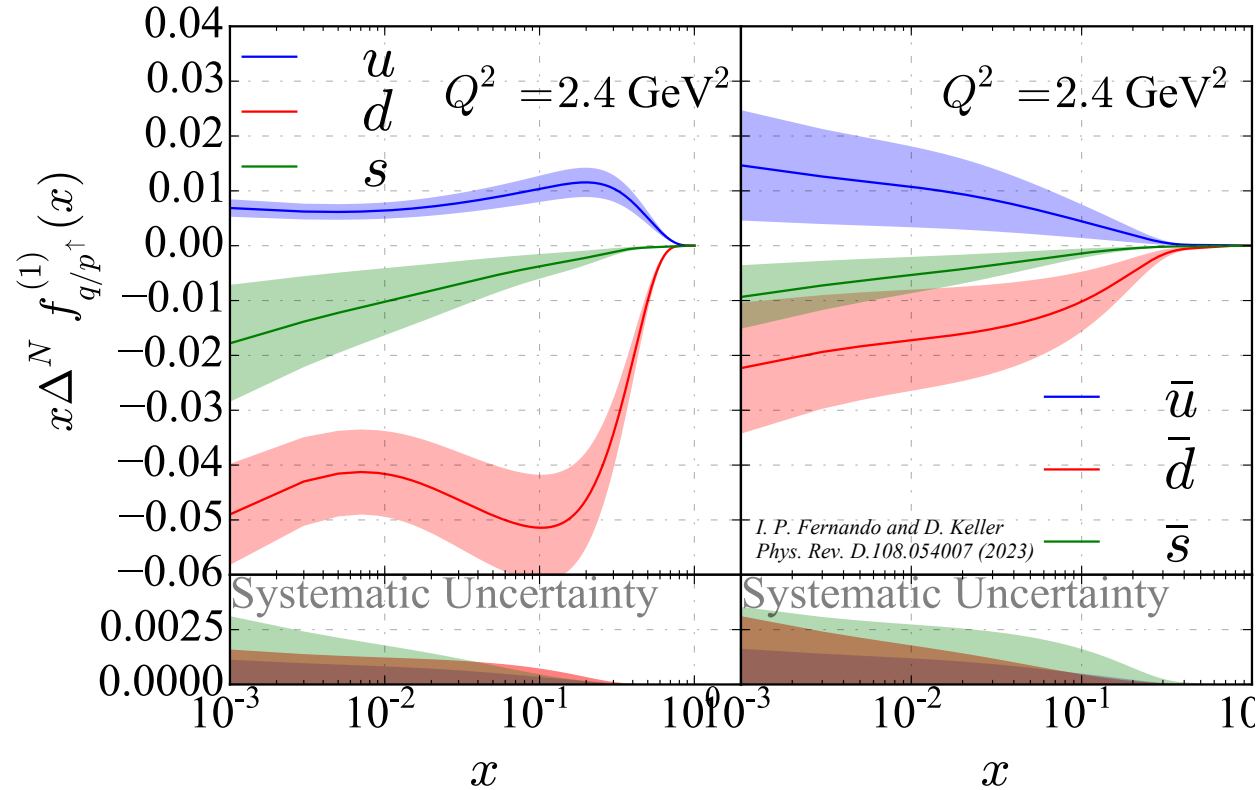
Calculated  $\chi_{\text{total}}^2/N_{\text{pt}} = 1.04$

# Sivers functions from the “Proton” DNN Model



# Sivers 1<sup>st</sup> moments from the “Proton” Model

$$\Delta^N f_{q/p^\uparrow}^{(1)}(x) = \int d^2 k_\perp \frac{k_\perp}{4m_p} \Delta^N f_{q/p^\uparrow}(x, k_\perp) = -f_{1T}^{\perp(1)q}(x)$$

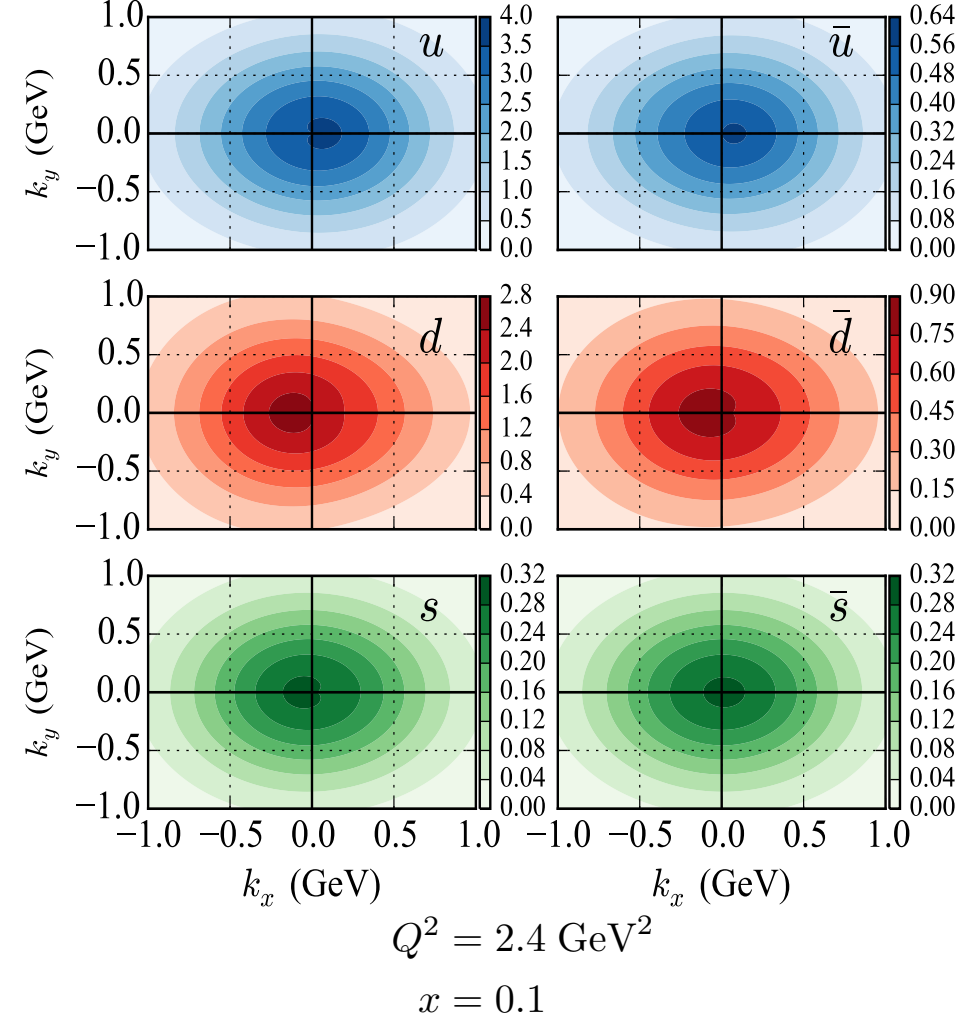


# 3D Tomography from the “Proton” DNN Model

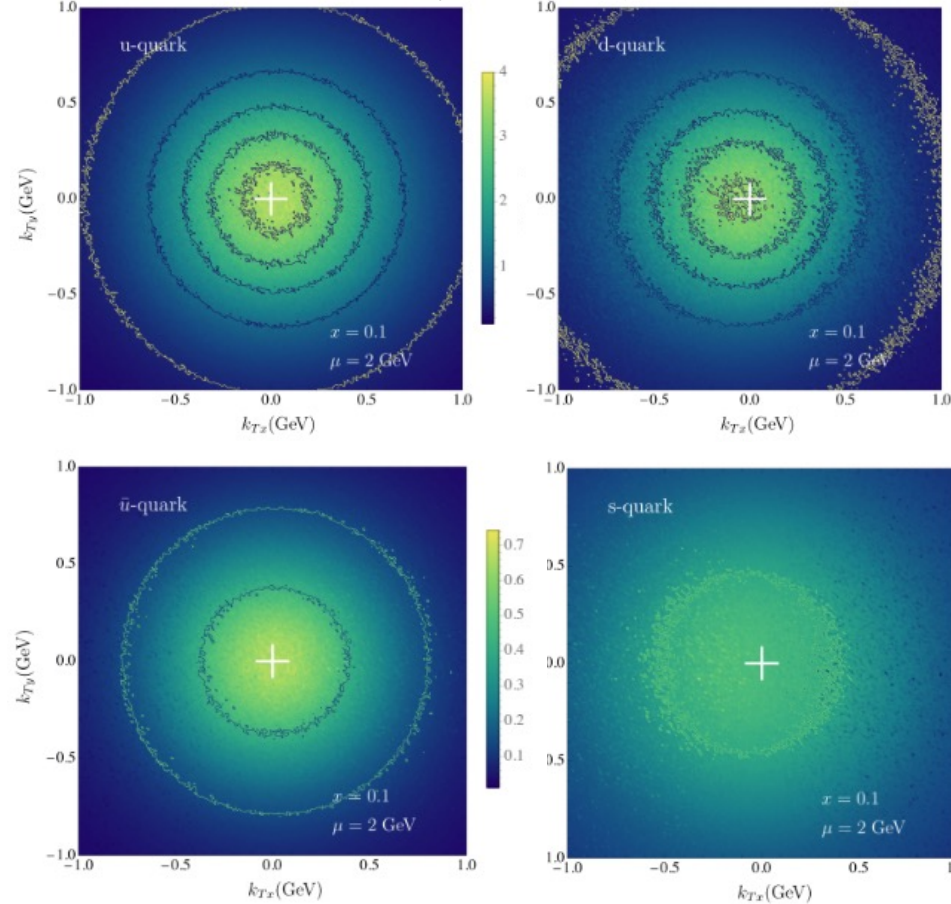
$$\rho_{p\uparrow}^a(x, k_x, k_y; Q^2) = f_1^a(x, k_\perp^2; Q^2) - \frac{k_x}{m_p} f_{1T}^a(x, k_\perp^2; Q^2)$$

I. P. Fernando and D. Keller  
Phys. Rev. D.108.054007 (2023)

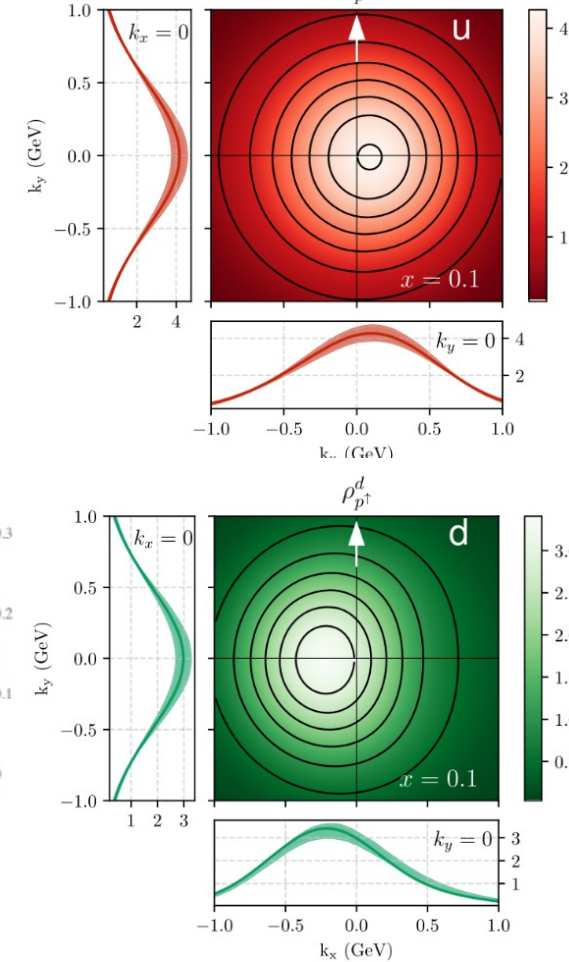
Proton-DNN model



Bury et al (2021)



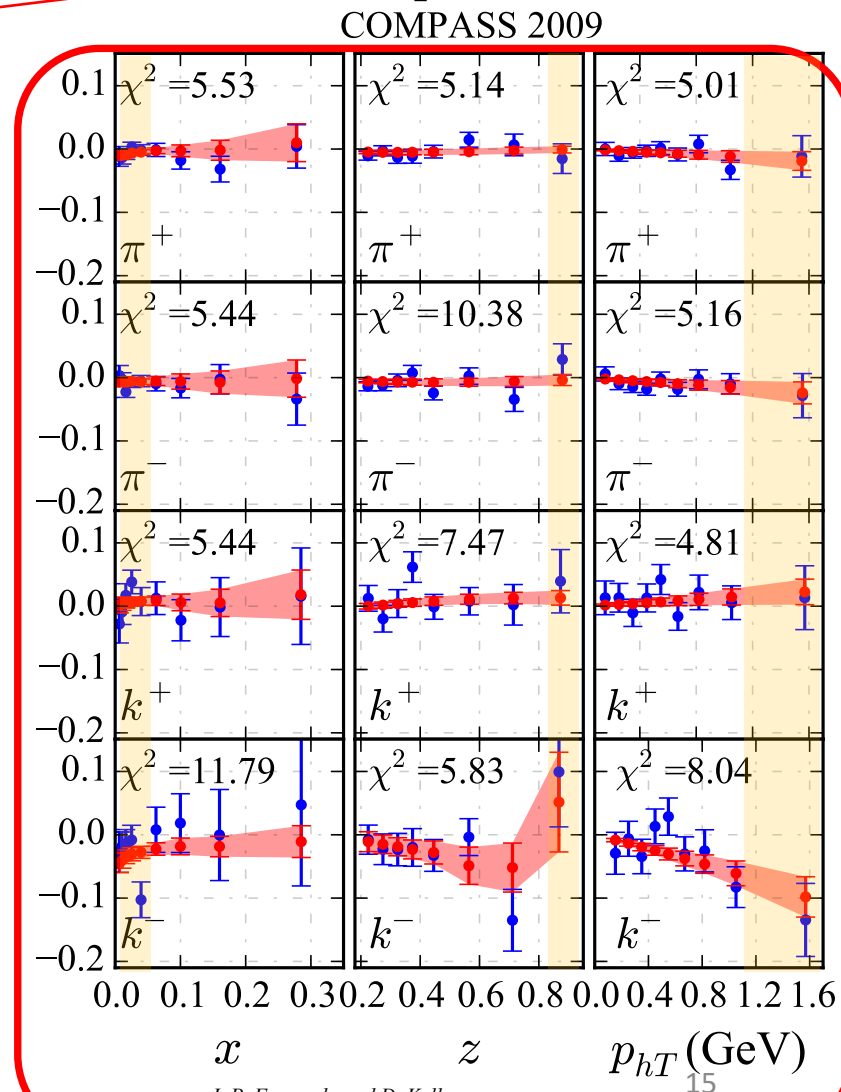
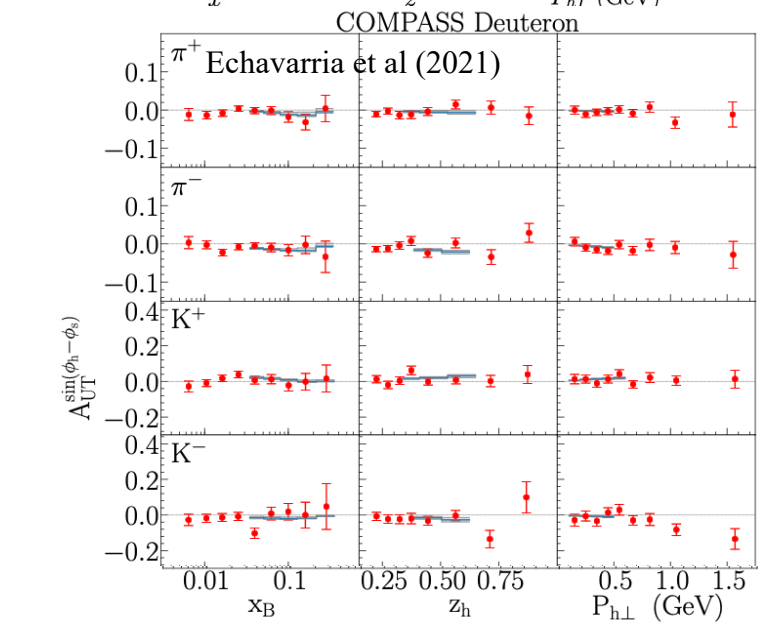
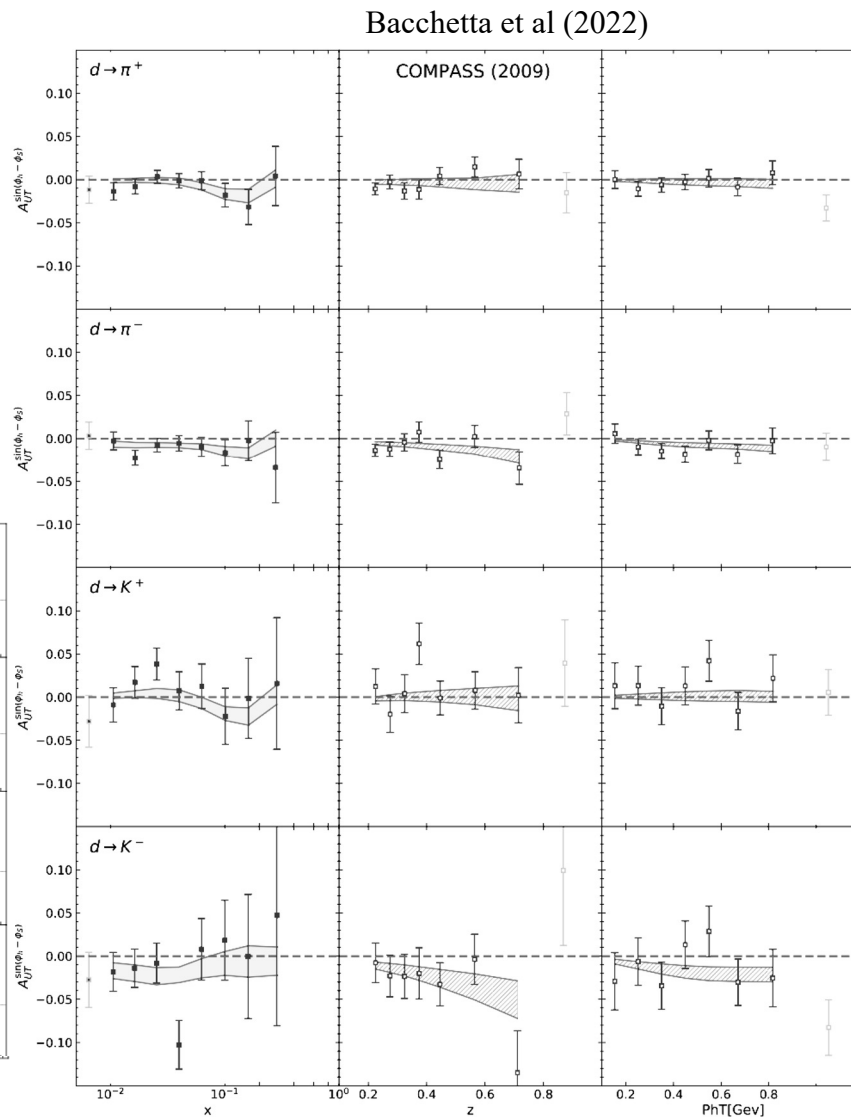
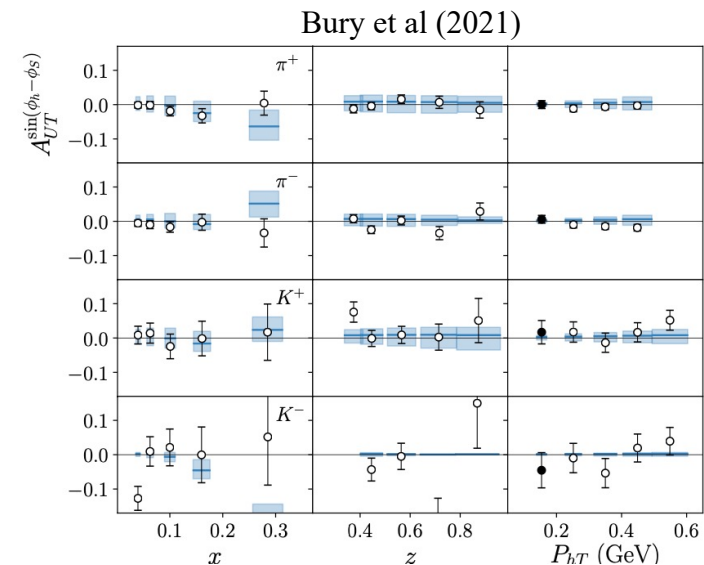
A. Bacchetta et al (2021)  $\rho_{p\uparrow}^u$



# Deuteron DNN Fit Results

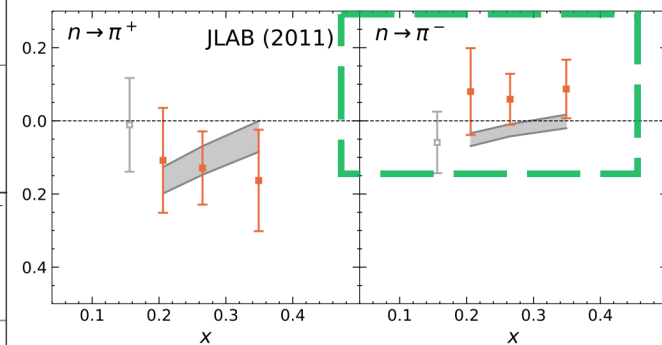
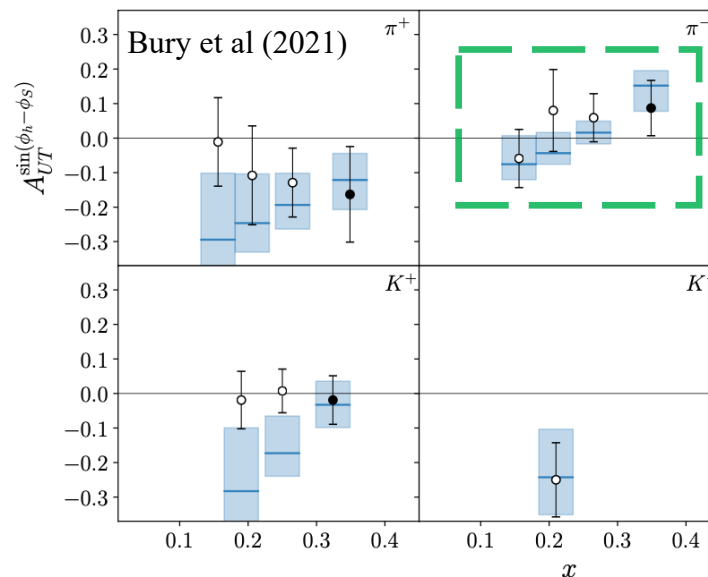
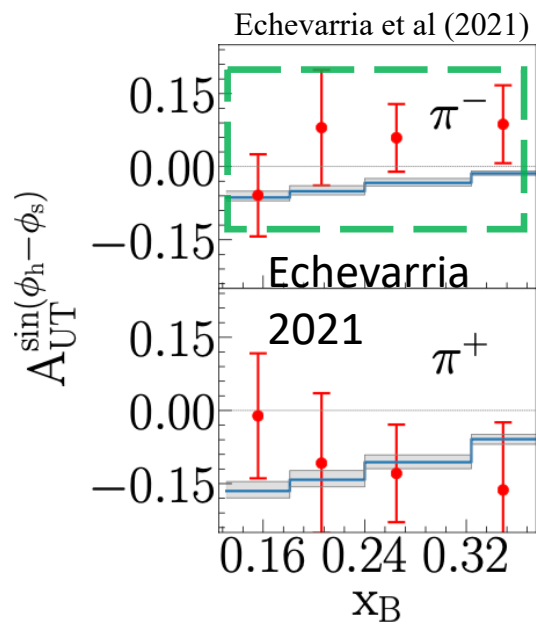
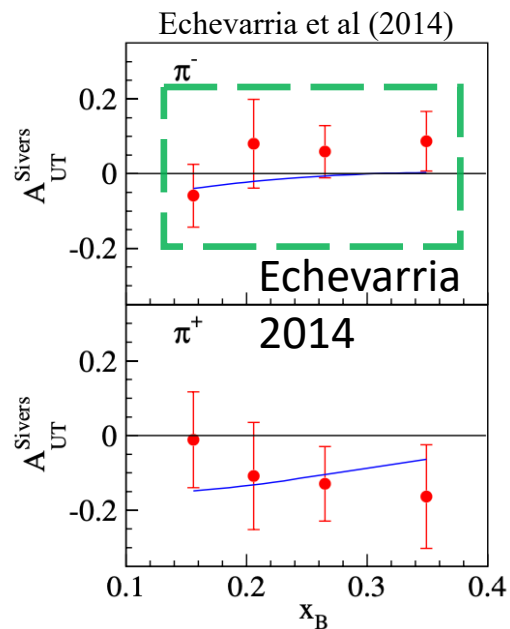
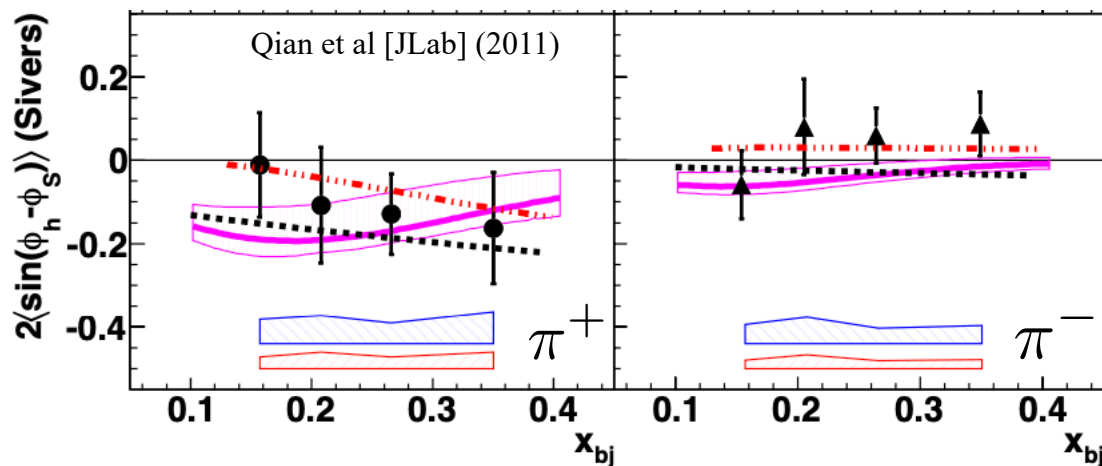
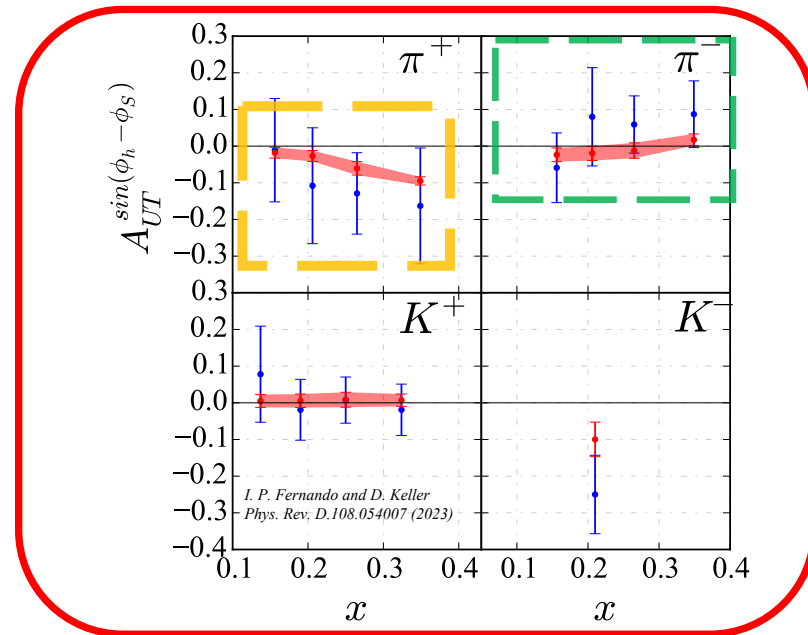
- No kinematic cuts are applied  
Deuteron-DNN model can describe data reasonably well
- No iso-spin symmetry conditions are applied

$$f_{1T,u\leftarrow d}^\perp = f_{1T,d\leftarrow d}^\perp = \frac{f_{1T,u\leftarrow p}^\perp + f_{1T,d\leftarrow p}^\perp}{2} \quad \chi^2/N_{\text{pt}} = 0.81$$



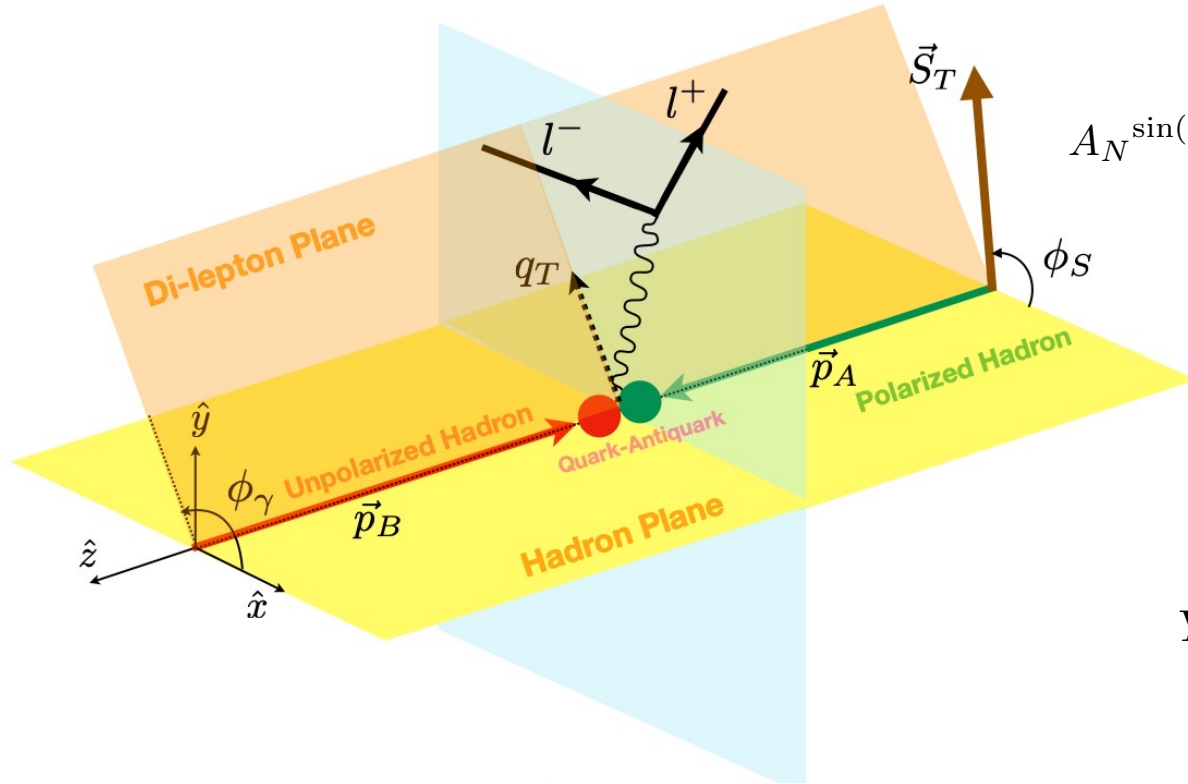
# Deuteron DNN Projections for JLab Kinematics

Deuteron-DNN



Bacchetta et al (2022)

# DNN Model Projections: DY



Anselmino et al. (2017)

$$A_N^{\sin(\phi_\gamma - \phi_S)}(x_F, M, q_T) = \mathcal{B}_0(q_T, m_1) \frac{\sum_q \frac{e_q^2}{x_1 + x_2} \mathcal{N}_q(x_1) f_{q/A}(x_1) f_{\bar{q}/B}(x_2)}{\sum_q \frac{e_q^2}{x_1 + x_2} f_{q/A}(x_1) f_{\bar{q}/B}(x_2)}$$

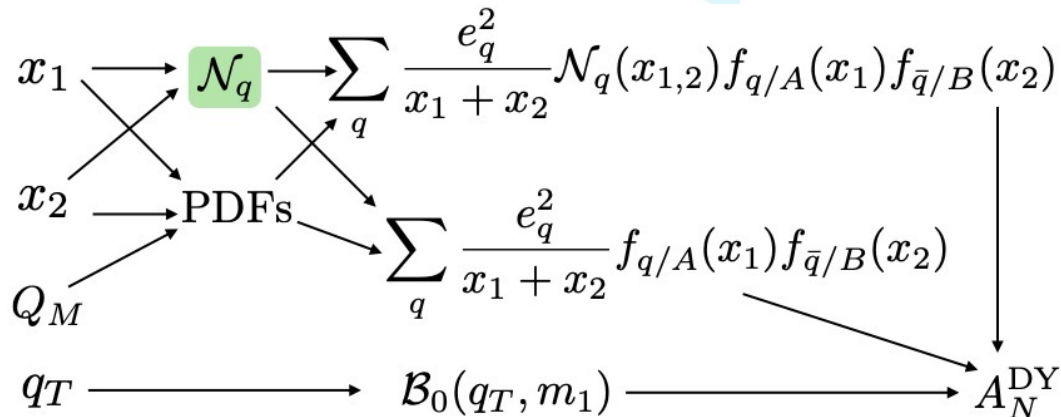
$$\mathcal{B}_0(q_T, m_1) = \frac{q_T \sqrt{2e}}{m_1} \frac{Y_1(q_T, k_S, k_{\perp 2})}{Y_2(q_T, k_{\perp 1}, k_{\perp 2})}$$

$$Y_1(q_T, k_S, k_{\perp 2}) = \left( \frac{\langle k_S^2 \rangle^2}{\langle k_{\perp 2}^2 \rangle (\langle k_S^2 \rangle + \langle k_{\perp 2}^2 \rangle)^2} \right) \times \exp \left( \frac{-q_T^2}{\langle k_S^2 \rangle + \langle k_{\perp 2}^2 \rangle} \right)$$

$$Y_2(q_T, k_{\perp 1}, k_{\perp 2}) = \left( \frac{1}{\langle k_{\perp 1}^2 \rangle + \langle k_{\perp 2}^2 \rangle} \right) \times \exp \left( \frac{-q_T^2}{\langle k_{\perp 1}^2 \rangle + \langle k_{\perp 2}^2 \rangle} \right)$$

$$\frac{1}{\langle k_S^2 \rangle} = \frac{1}{m_1^2} + \frac{1}{\langle k_{\perp 1}^2 \rangle}$$

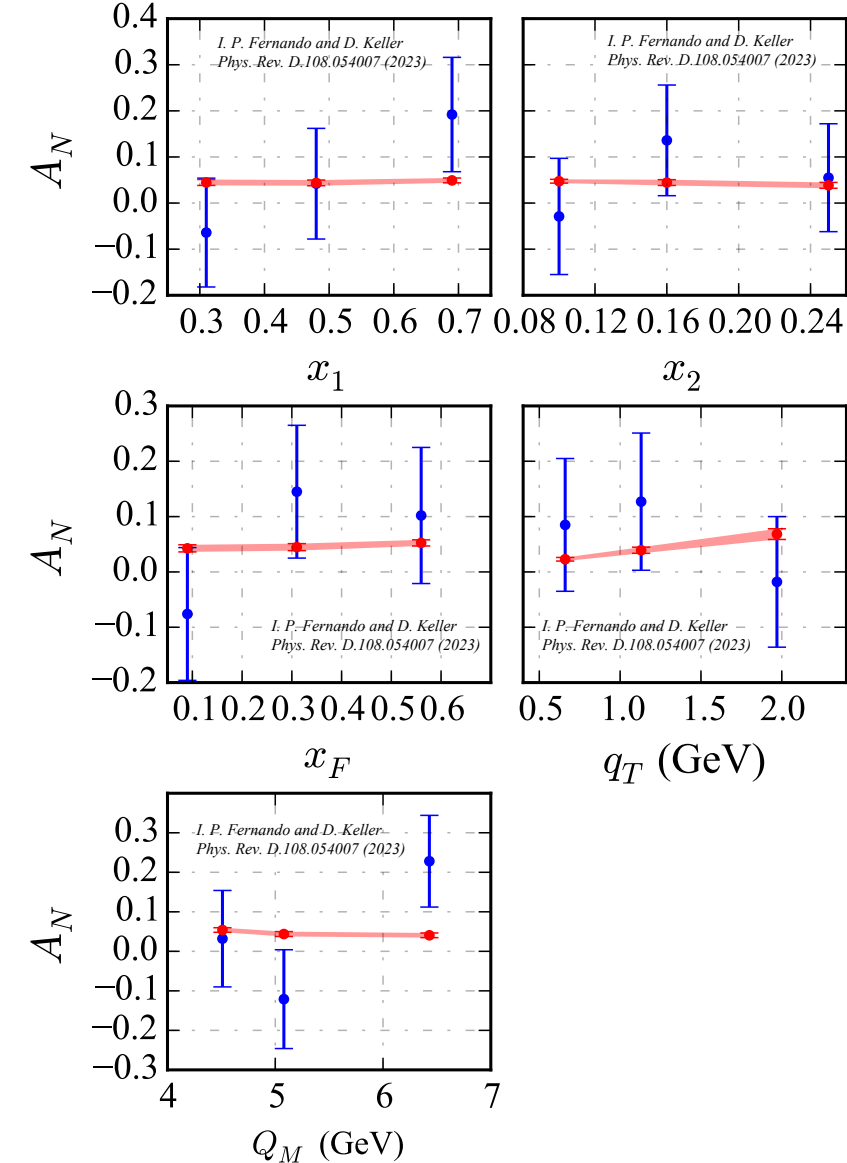
$$\langle k_{\perp 1}^2 \rangle = \langle k_{\perp 2}^2 \rangle = \langle k_{\perp}^2 \rangle = 0.25 \text{ GeV}^2$$



$$\Delta^N f_{q/p^\uparrow}(x, k_\perp)|_{\text{SIDIS}} = -\Delta^N f_{q/p^\uparrow}(x, k_\perp)|_{\text{DY}}$$

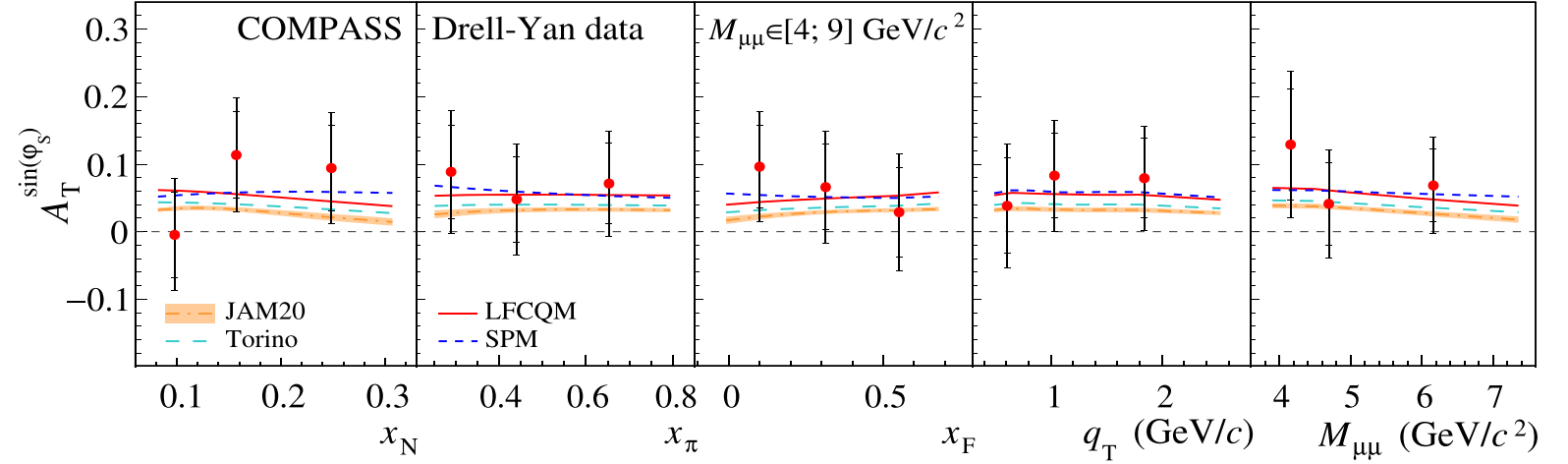
# DNN (Proton) Model Projections: DY

COMPASS 2017 DY Projections



COMPASS 2024

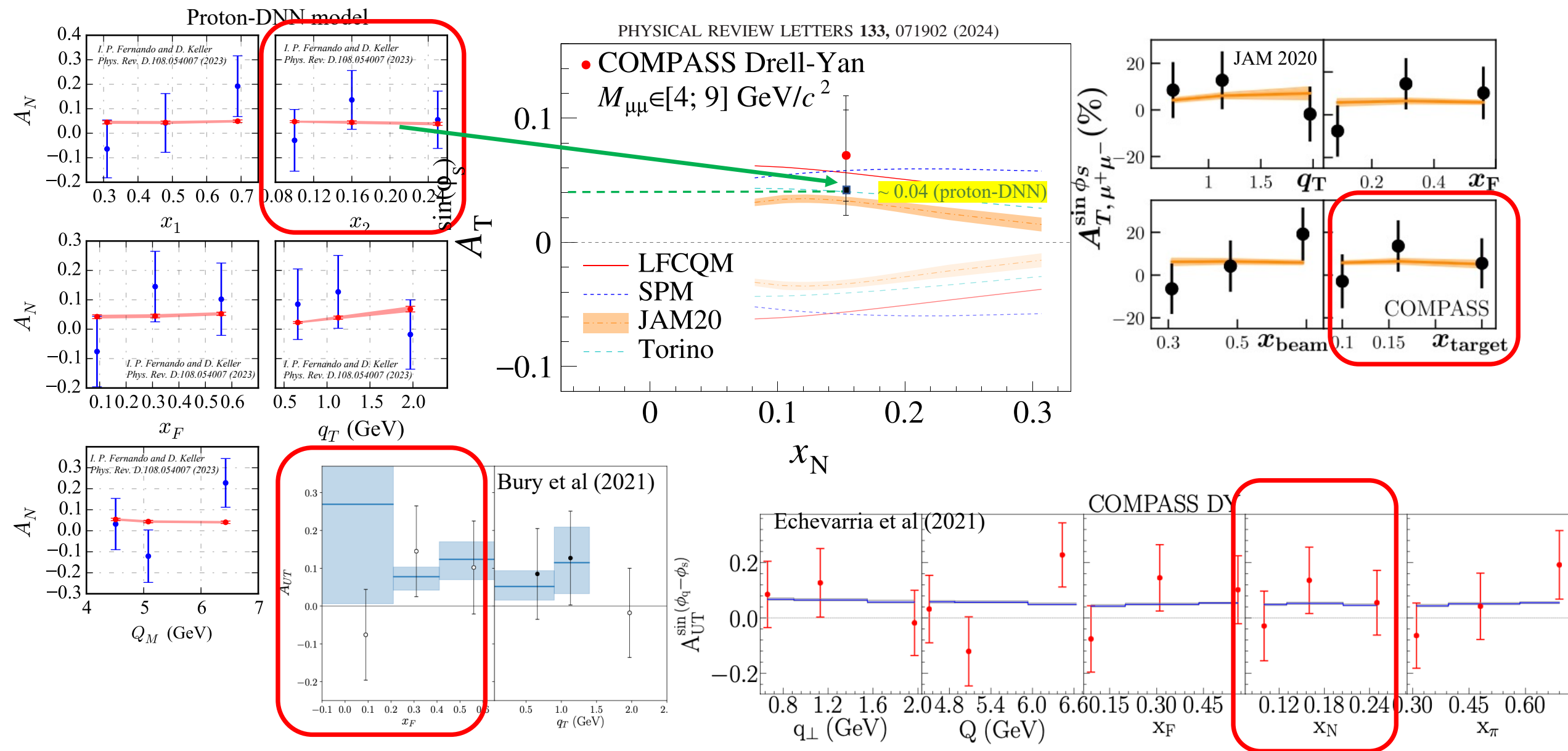
PHYSICAL REVIEW LETTERS **133**, 071902 (2024)



Note: These proton-DNN **projections** based on the assuming the sign-change of the Sivers functions

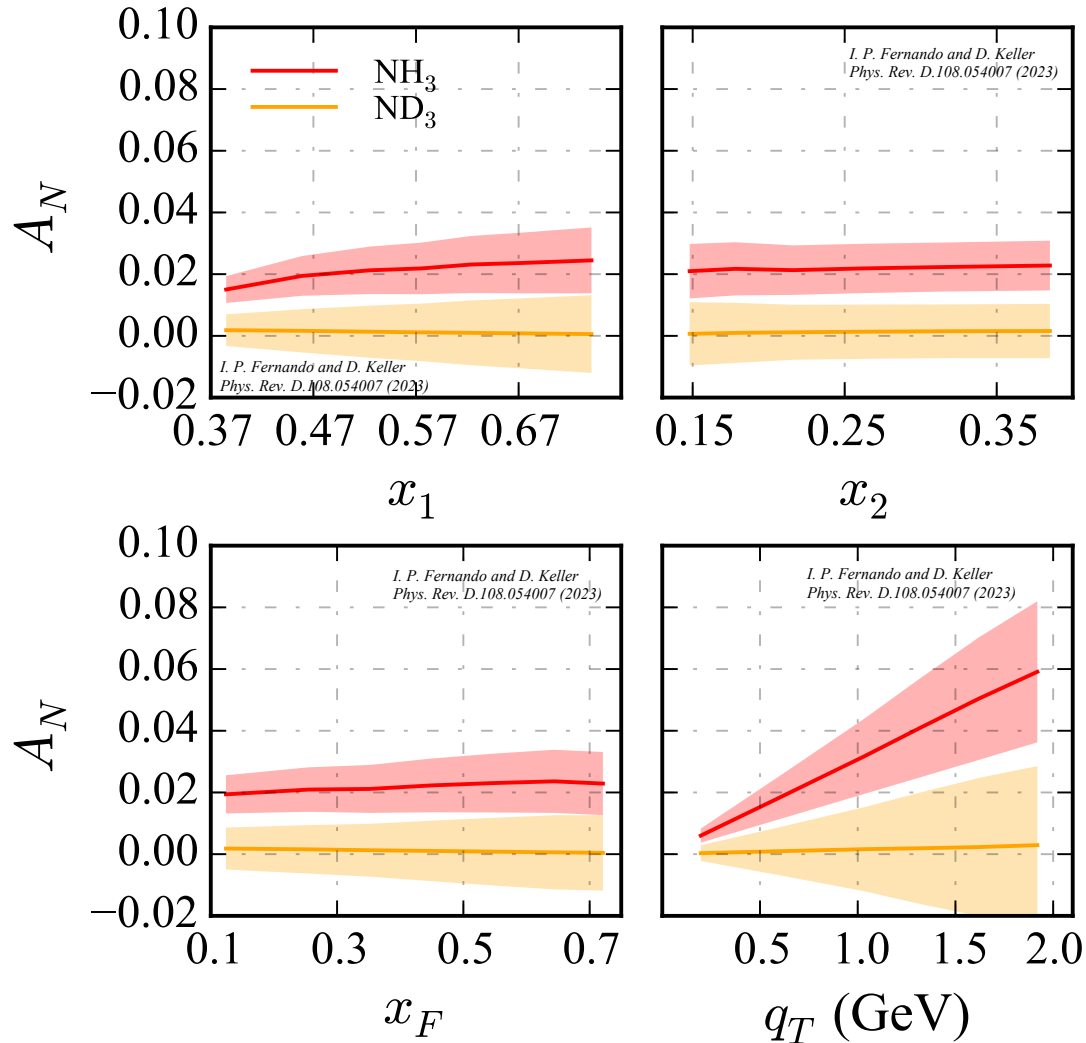
# DNN Model Projections: DY

In Comparison with COMPASS 2024 Final



# DNN Model Projections: DY @ SpinQuest

DNN Models



- SpinQuest (E1039) experiment at Fermilab is aiming to extract the Sivers function for the light-sea quarks.
- Unpolarized 120 GeV proton beam with polarized proton and deuteron targets (separately).
- Proton-DNN model predictions (Red)  
Deuteron-DNN model predictions (Orange)

# Systematic Studies: data cuts

$$\begin{aligned}
 W^{\mu\nu} = & \sum_f |\mathcal{H}_f(Q^2, \mu)|^{\mu\nu} \\
 & \times \int d^2 k_\perp d^2 p_\perp \delta^{(2)}(z_h k_\perp + p_\perp - p_{hT}) \\
 & \times F_{f/N^\uparrow}(x, z_h k_\perp, S; \mu, \zeta_F) D_{h/f}(z_h, p_\perp; \mu, \zeta_D) \\
 & + Y(p_{hT}, Q^2),
 \end{aligned}$$

Examples:

1. Bury et al JHEP 05 (2021) 151

$$Q > 2 \text{ GeV}$$

$$\delta = p_{hT}/zQ \leq 0.3$$

2. Echevarria et al JHEP 01 (2021) 126

$$q_T/Q < 0.75$$

3. JAM2020

$$Q^2 > 1.63 \text{ GeV}^2, \quad 0.2 < z < 0.6, \quad 0.2 < p_{hT} < 0.9 \text{ GeV}$$

So far, the applicability of TMD factorization was ensured by applying cuts to SIDIS data based on various criteria in the literature.

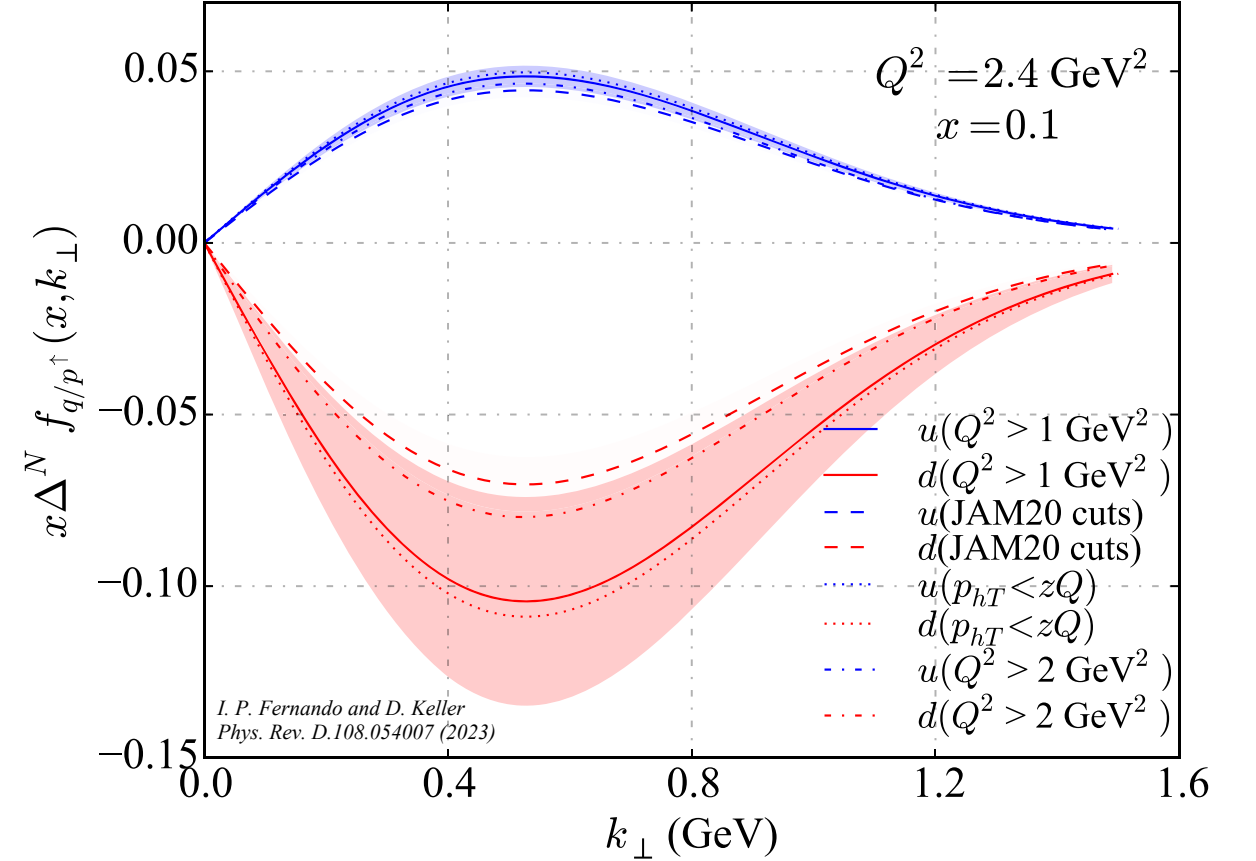
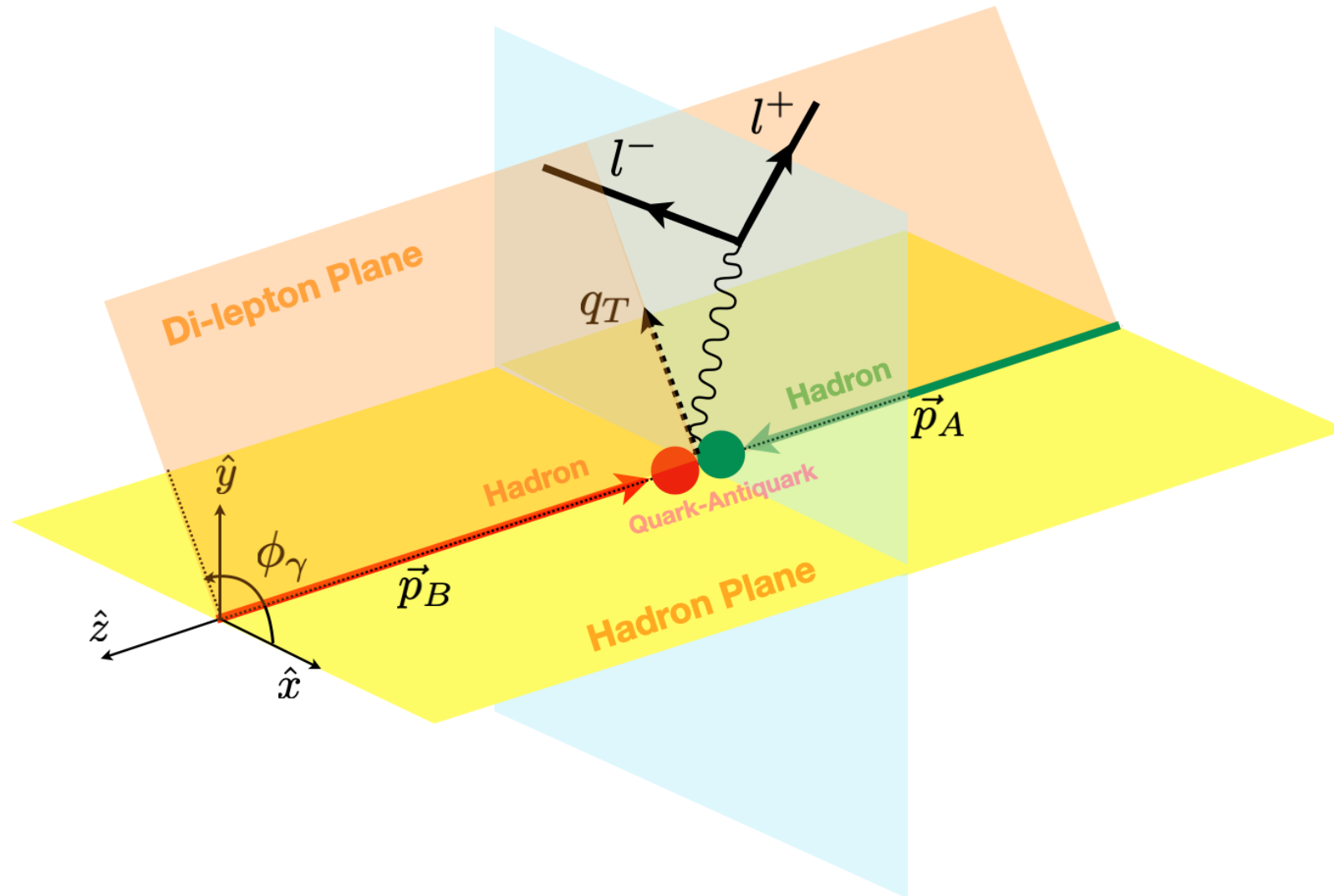


FIG. 17. Solid lines with light band represent the  $u$  (in blue),  $d$  (in red) parton distribution functions using the cut  $Q^2 > 1 \text{ GeV}^2$ . These resulting DNN models made from the cuts from all tests are also shown.

# Unpolarized TMDs with fixed target DY data



# Unpolarized TMDs: Motivation

- Can we obtain TMDs directly in  $\mathbf{k}_T$  space instead of  $\mathbf{b}_T$ -space?

We are interested in both. We think having a framework with  $\mathbf{k}_T$  and complementary to  $\mathbf{b}_T$  space

$$\frac{d\sigma}{dq_T dQ_M dy} = \frac{16\pi^2 \alpha^2}{9Q_M^3} q_T \sum_q e_q^2 \mathcal{H}^{DY} \int d^2\mathbf{k}_{aT} d^2\mathbf{k}_{bT} f_{q/a}(x_a, \mathbf{k}_{aT}; \mu_Q, Q^2) f_{\bar{q}/b}(x_b, \mathbf{k}_{bT}; \mu_Q, Q^2) \delta^{(2)}(\mathbf{q}_T - \mathbf{k}_{aT} - \mathbf{k}_{bT}) + (x_a \leftrightarrow x_b)$$

- Number of data points vs cuts:  
Our goal is to use as much data as available while TMD factorization is still valid.
- Different types of parameterizations attempted in the literature:  
So, we want to explore a purely numerical approach utilizing DNNs

# Unpolarized TMDs: Setup

Introducing (exploration of) a separable form

$$f_q(x, k_\perp, Q_M) = \boxed{f_q(x, Q_M)} \boxed{s(x, k_\perp)} \boxed{\mathcal{B}(Q_M)}$$

Collinear-PDFs with  
DGLAP Evolution

Transvers Momentum Kernal  
(DNN)

Transvers Momentum Evolution Kernal  
(DNN)

$$\hat{f}_1^a(x, \mathbf{b}_T^2; \mu_f, \zeta_f) = \hat{f}_1^a(x, \mathbf{b}_T^2; \mu_i, \zeta_i) \exp \left\{ \int_{\mu_i}^{\mu_f} \frac{d\mu}{\mu} \gamma(\mu, \zeta_f) \right\} \left( \frac{\zeta_f}{\zeta_i} \right)^{K(|\mathbf{b}_T|, \mu_i)/2}$$

$$\frac{d\sigma}{dq_T dQ_M dy} = \frac{16\pi^2 \alpha^2}{9Q_M^3} q_T \sum_q e_q^2 \mathcal{H}^{DY} \int d^2 \mathbf{k}_{aT} d^2 \mathbf{k}_{bT} f_{q/a}(x_a, \mathbf{k}_{aT}; \mu_Q, Q^2) f_{\bar{q}/b}(x_b, \mathbf{k}_{bT}; \mu_Q, Q^2) \delta^{(2)}(\mathbf{q}_T - \mathbf{k}_{aT} - \mathbf{k}_{bT}) + (x_a \leftrightarrow x_b)$$

$$\frac{d\sigma}{dq_T dQ_M dy} = \frac{16\pi^2 \alpha^2}{9Q_M^3} q_T \sum_q e_q^2 x_a f_q(x_a, Q_M) x_b f_{\bar{q}}(x_b, Q_M) \mathcal{S}(q_T, x_a, x_b) \mathcal{B}^2(Q_M) + (x_a \leftrightarrow x_b)$$

# Unpolarized TMDs: Setup

Introducing (exploration of) a separable form

$$f_q(x, k_\perp, Q_M) = f_q(x, Q_M) s(x, k_\perp) \mathcal{B}(Q_M)$$

Collinear-PDFs with  
DGLAP Evolution

Transvers Momentum Kernal

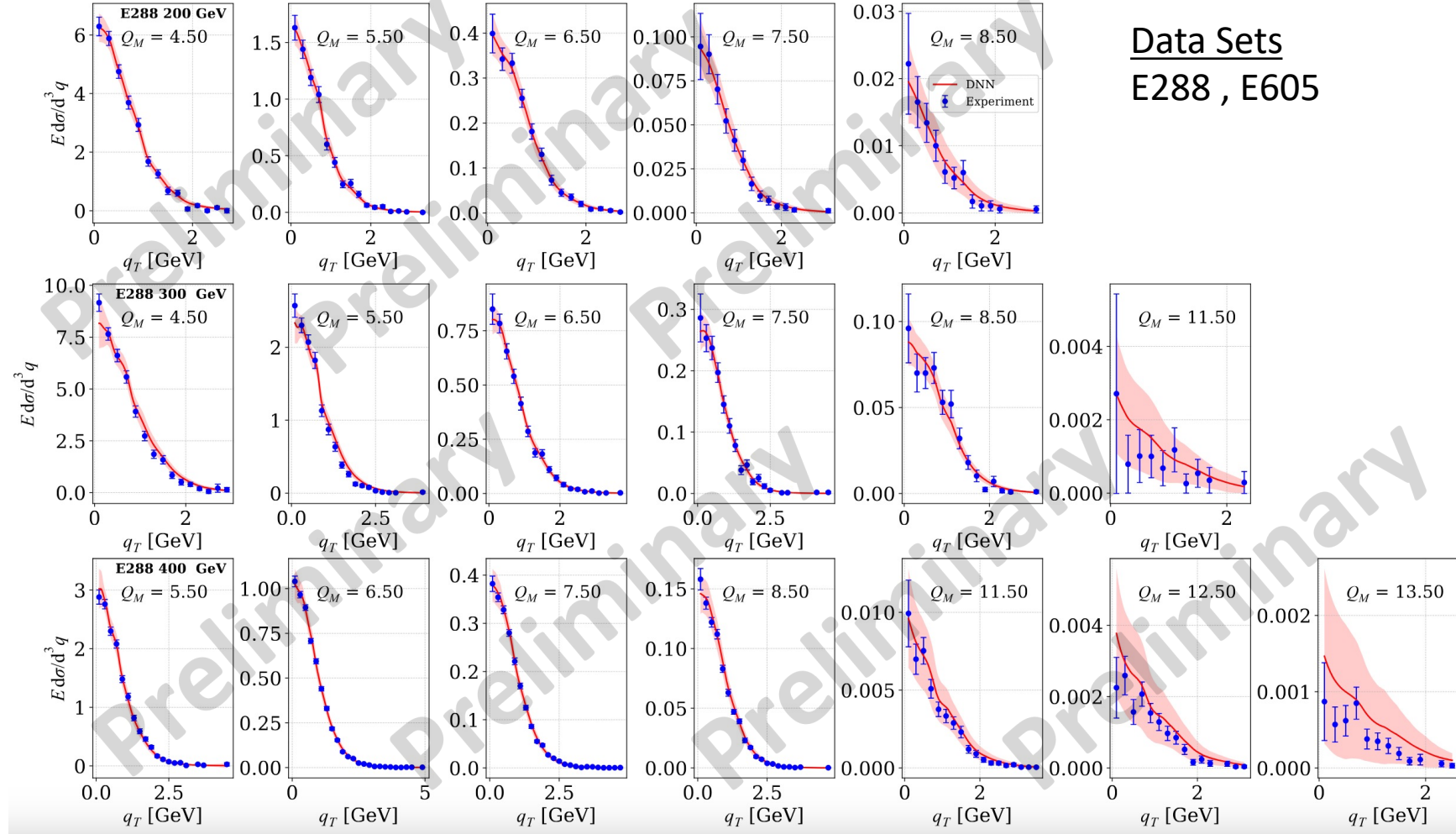
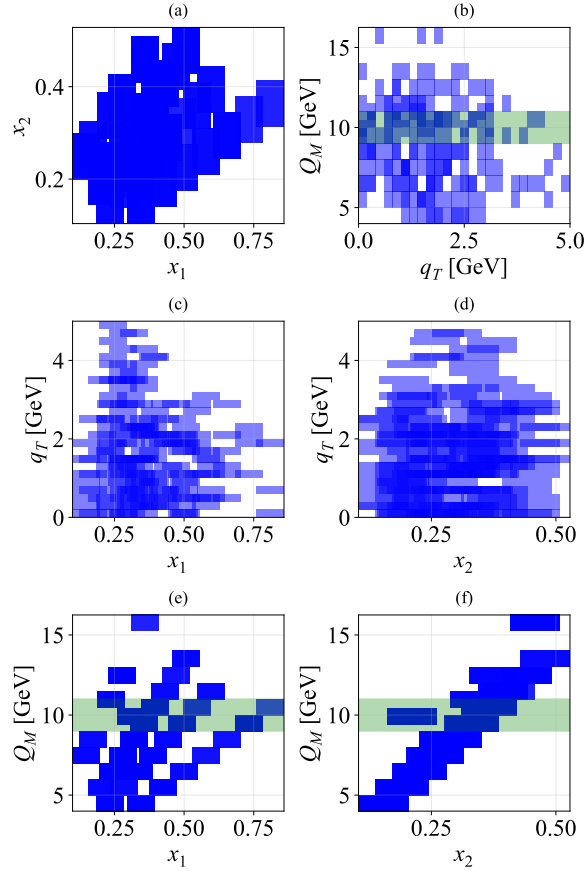
Transvers Momentum Evolution Kernal

$$\frac{d\sigma}{dq_T dQ_M dy} = \frac{16\pi^2 \alpha^2}{9Q_M^3} q_T \sum_q e_q^2 \mathcal{H}^{DY} \int d^2 \mathbf{k}_{aT} d^2 \mathbf{k}_{bT} f_{q/a}(x_a, \mathbf{k}_{aT}; \mu_Q, Q^2) f_{\bar{q}/b}(x_b, \mathbf{k}_{bT}; \mu_Q, Q^2) \delta^{(2)}(\mathbf{q}_T - \mathbf{k}_{aT} - \mathbf{k}_{bT}) + (x_a \leftrightarrow x_b)$$

$$\frac{d\sigma}{dq_T dQ_M dy} = \frac{16\pi^2 \alpha^2}{9Q_M^3} q_T \sum_q e_q^2 x_a f_q(x_a, Q_M) x_b f_{\bar{q}}(x_b, Q_M) \mathcal{S}(q_T, x_a, x_b) \mathcal{B}^2(Q_M) + (x_a \leftrightarrow x_b)$$

$$\mathcal{S}(q_T, x_a, x_b) = \int_0^\infty dk_\perp k_\perp \int_0^{2\pi} d\phi s(x_a, k_\perp) s\left(x_b, \sqrt{q_T^2 + k_\perp^2 - 2q_T k_\perp \cos \phi}\right)$$

# Current Status



Data Sets  
E288 , E605

$$S(q_T, x_a, x_b) = \int_0^\infty dk_\perp k_\perp \int_0^{2\pi} d\phi s(x_a, k_\perp) s\left(x_b, \sqrt{q_T^2 + k_\perp^2 - 2q_T k_\perp \cos \phi}\right)$$

$$f_q(x; Q) = \int d^2 k_\perp f_q(x, k_\perp; Q)$$

Finalizing the simultaneous fits to obtain the TMDs (flavor dependent)

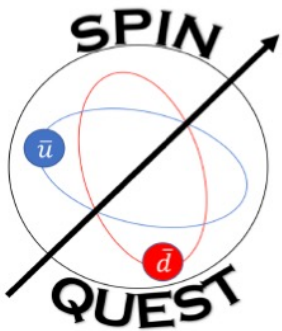
$$f_q(x, k_\perp, Q_M) = f_q(x, Q_M) s(x, k_\perp) \mathcal{B}(Q_M)$$

# Summary & Outlook

- We proposed a method for performing global fits to extract TMDs employing DNNs (first-ever application of DNNs in extracting TMDs).
- Extracting Sivers function was performed as an example of this method based on utilizing DNNs
- We have successfully tested our method with pseudo-data, also a dedicated systematic study.
- We projected SIDIS and DY Sivers asymmetries:  
for already completed experiments (as a validation check: COMPASS) and  
upcoming experiments (such as SpinQuest).
- Currently working on Unpolarized TMDPDF extraction...

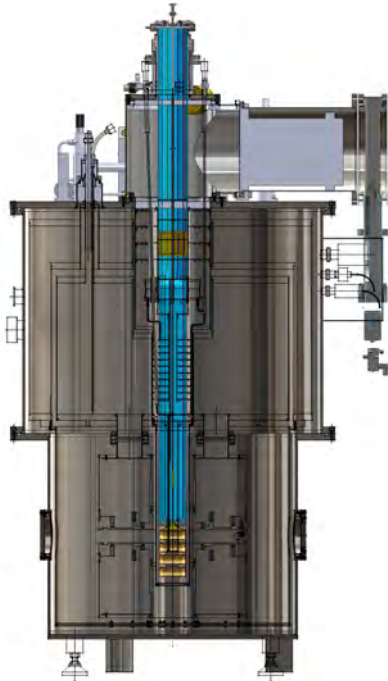
Next:

- Applying the “DNN method” to extract other TMDs such as Transversity, Boer-Mulders function, as well as Spin-1 TMDs.
- Make projections to EIC kinematics



# SpinQuest (E1039) Experiment at Fermilab

- Probing Sivers asymmetry from the (light) 'sea' quark contributions



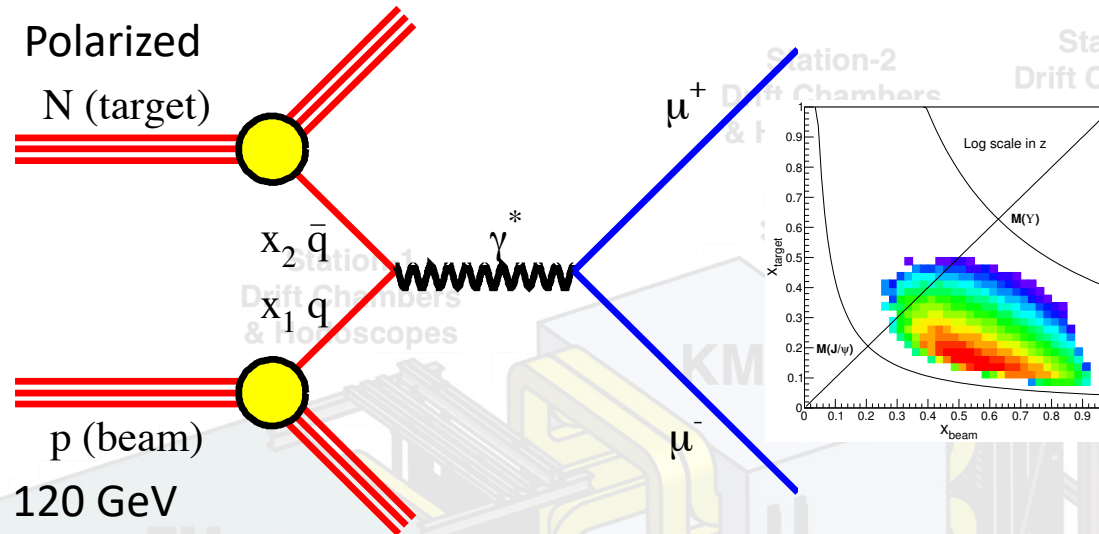
LANL-UVA

Polarized Target

<https://spinqwest.fnal.gov/>

<http://twist.phys.virginia.edu/E1039/>

$$pp^\uparrow(d^\uparrow) \rightarrow \mu^+\mu^-X, 4 < M_{\mu\mu} < 9 \text{ GeV}$$

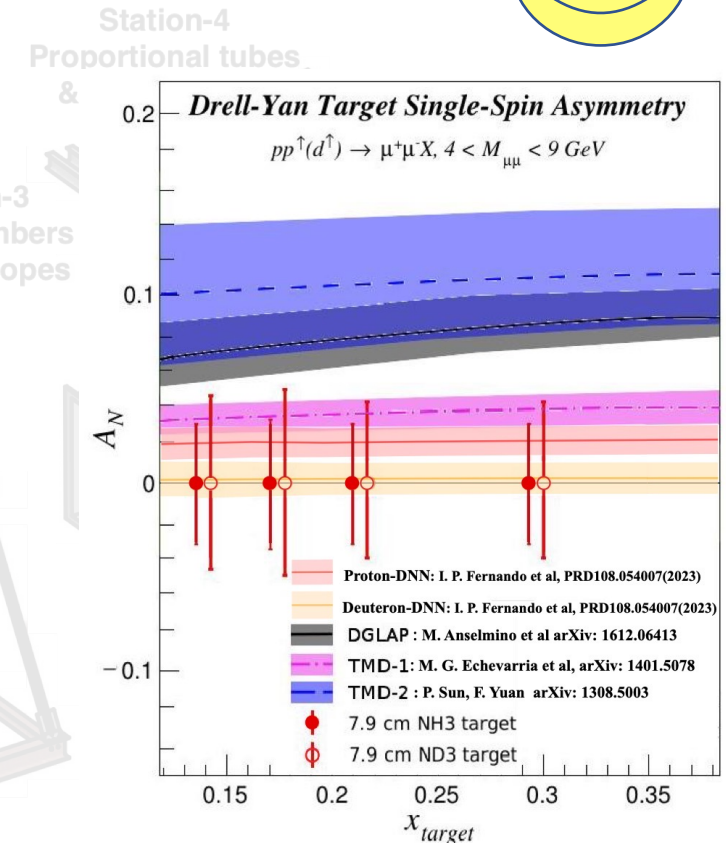


$$\frac{d\sigma}{dx_1 dx_2} = \frac{4\pi\alpha^2}{9sx_1 x_2} \sum_i e_i^2 (q_i^B(x_1, Q^2) \bar{q}_i^T(x_2, Q^2) + \bar{q}_i^B(x_1, Q^2) q_i^T(x_2, Q^2))$$

Please Join The Effort

Dustin Keller ([dustin@virginia.edu](mailto:dustin@virginia.edu))[Spokesperson]

Kun Liu ([liuk@lanl.gov](mailto:liuk@lanl.gov))[Spokesperson]]



Highest beam intensity on a polarized target ever!

*Thank you*

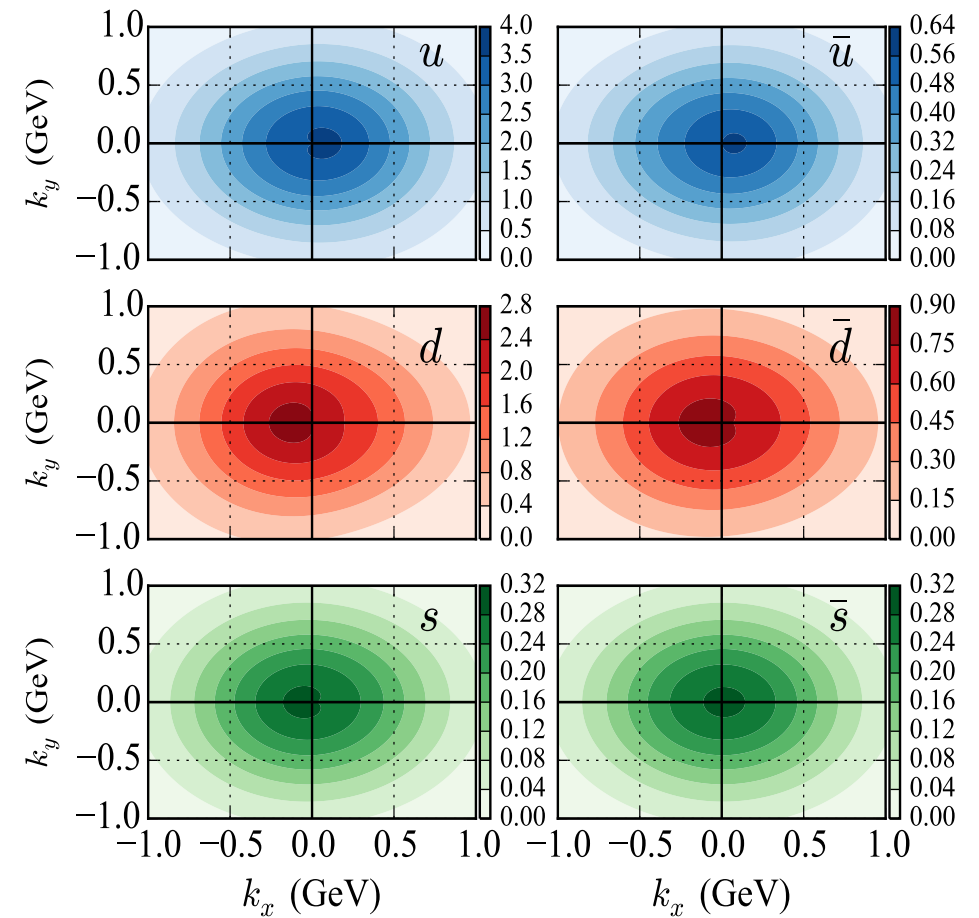


UNIVERSITY  
*of* VIRGINIA



U.S. DEPARTMENT OF  
**ENERGY**

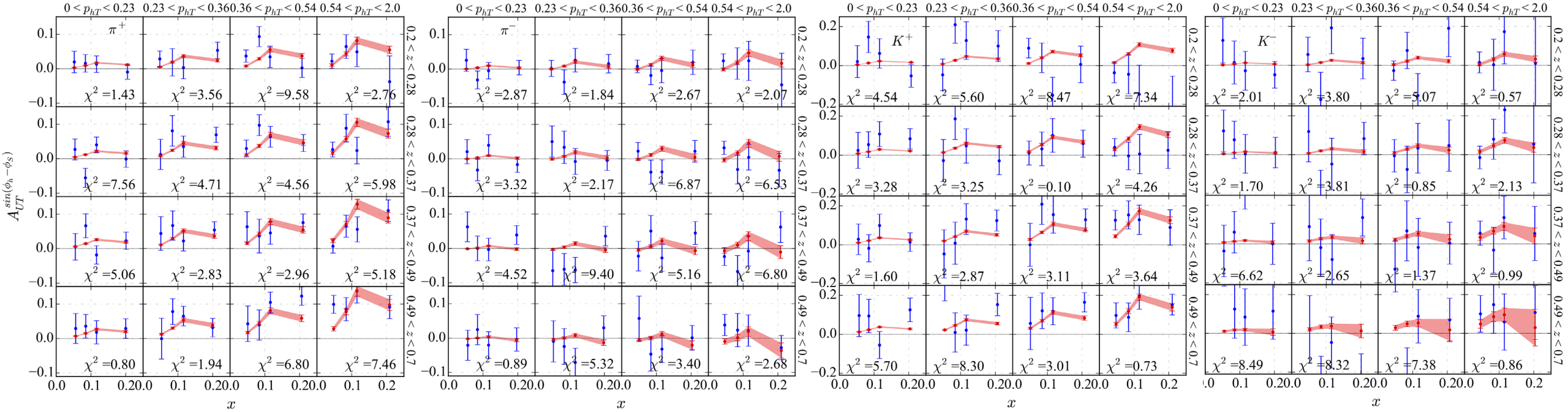
Office of  
Science



This work is supported by DOE contract DE-FG02-96ER40950

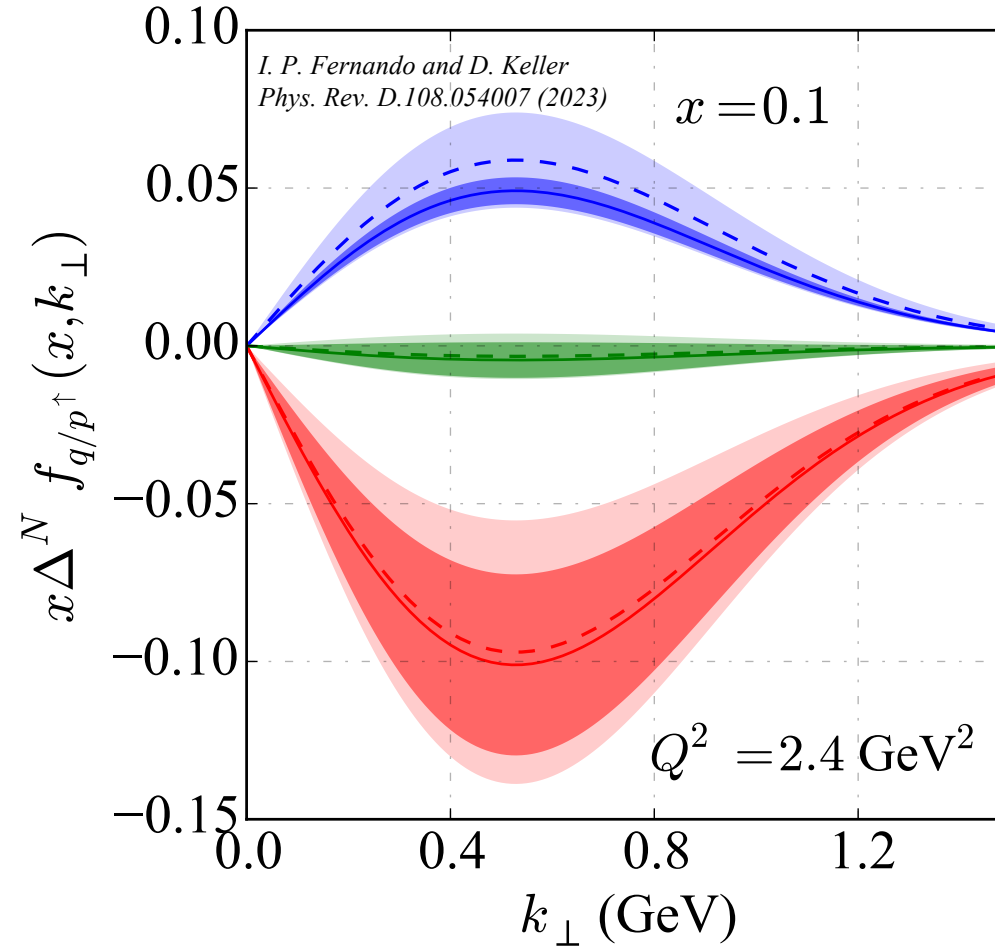
# *Backup Slides*

# Projections from the ‘Proton’ DNN Model



Projections of the of HERMES 2020 data for 3D kinematic bins, using the proton-DNN model including 68% C.L. error bands (in red) in comparison with the actual data points (in blue).

# DNN Method: With Real data (Quality of the extraction)



The qualitative improvement of the extracted Sivers functions for u (blue), d (red), and s (green) quarks at  $x = 0.1$  and  $Q^2 = 2.4 \text{ GeV}^2$  using the optimized proton-DNN model at the Second Iteration (solid-lines with dark-colored error bands with 68% CL), compared to the First Iteration (dashed-lines with light-colored error bands with 68% CL)

# Systematic Studies: Choice of $h(k)$

$$\Delta^N f_{q/p^\uparrow}(x, k_\perp) = 2\mathcal{N}_q(x)h(k_\perp)f_{q/p}(x, k_\perp)$$

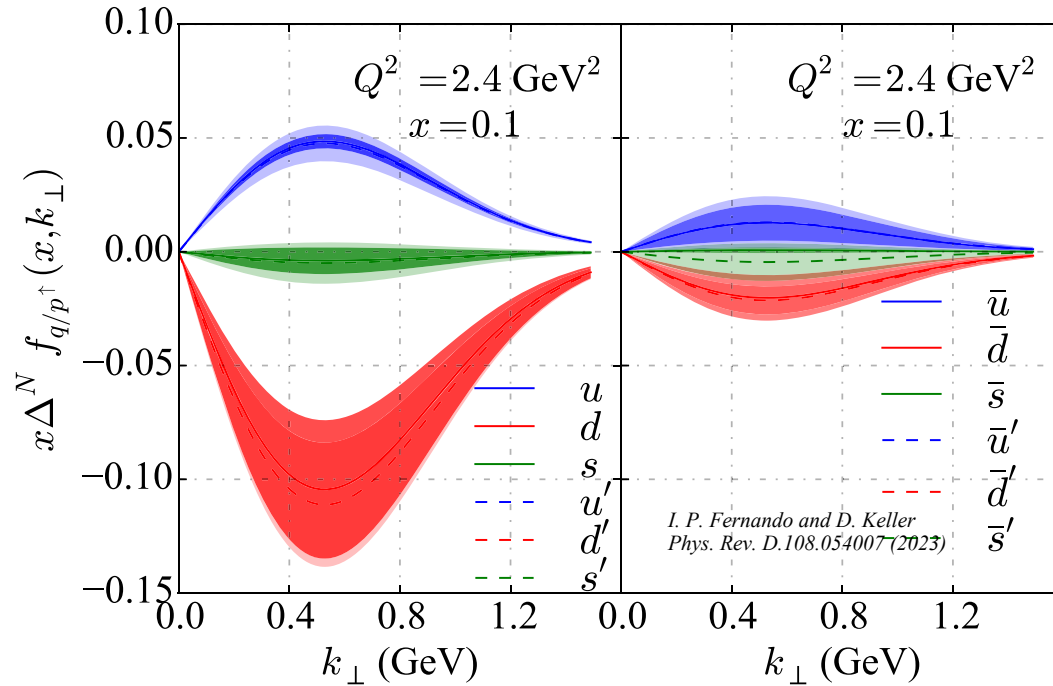


FIG. 19. Using two different  $h(k_\perp)$ . Solid line with dark band represents the Siverts functions with  $h(k_\perp) = \sqrt{2}e \frac{k_\perp}{m_1} e^{-k_\perp^2/m_1^2}$ , whereas the dashed line with light band represents the Siverts functions with  $h(k_\perp) = \frac{2k_\perp m_1}{m_1^2 + k_\perp^2}$ .

$$h(k_\perp) = \sqrt{2}e \frac{k_\perp}{m_1} e^{-k_\perp^2/m_1^2}$$

$$h(k_\perp) = \frac{2k_\perp m_1}{m_1^2 + k_\perp^2}$$

- It is clear that the DNN is capable of incorporating both types of  $h(k)$  without affecting the Siverts functions in the final model as well as the asymmetries (with deviation less than 1%).
- This is because DNN demonstrates that it maps to the  $h(k)$  such that the Siverts function is nearly unchanged.

# Systematic Studies: data cuts

$$\begin{aligned}
 W^{\mu\nu} = & \sum_f |\mathcal{H}_f(Q^2, \mu)|^{\mu\nu} \\
 & \times \int d^2 k_\perp d^2 p_\perp \delta^{(2)}(z_h k_\perp + p_\perp - p_{hT}) \\
 & \times F_{f/N^\uparrow}(x, z_h k_\perp, S; \mu, \zeta_F) D_{h/f}(z_h, p_\perp; \mu, \zeta_D) \\
 & + Y(p_{hT}, Q^2),
 \end{aligned}$$

In addition to the basic data cut  $Q^2 > 1 \text{ GeV}^2$  we performed  $Q^2 > 2 \text{ GeV}^2$  and  $p_{hT} < zQ$  cuts separately with the proton-DNN model to understand the impact on the extracted Sivers functions.

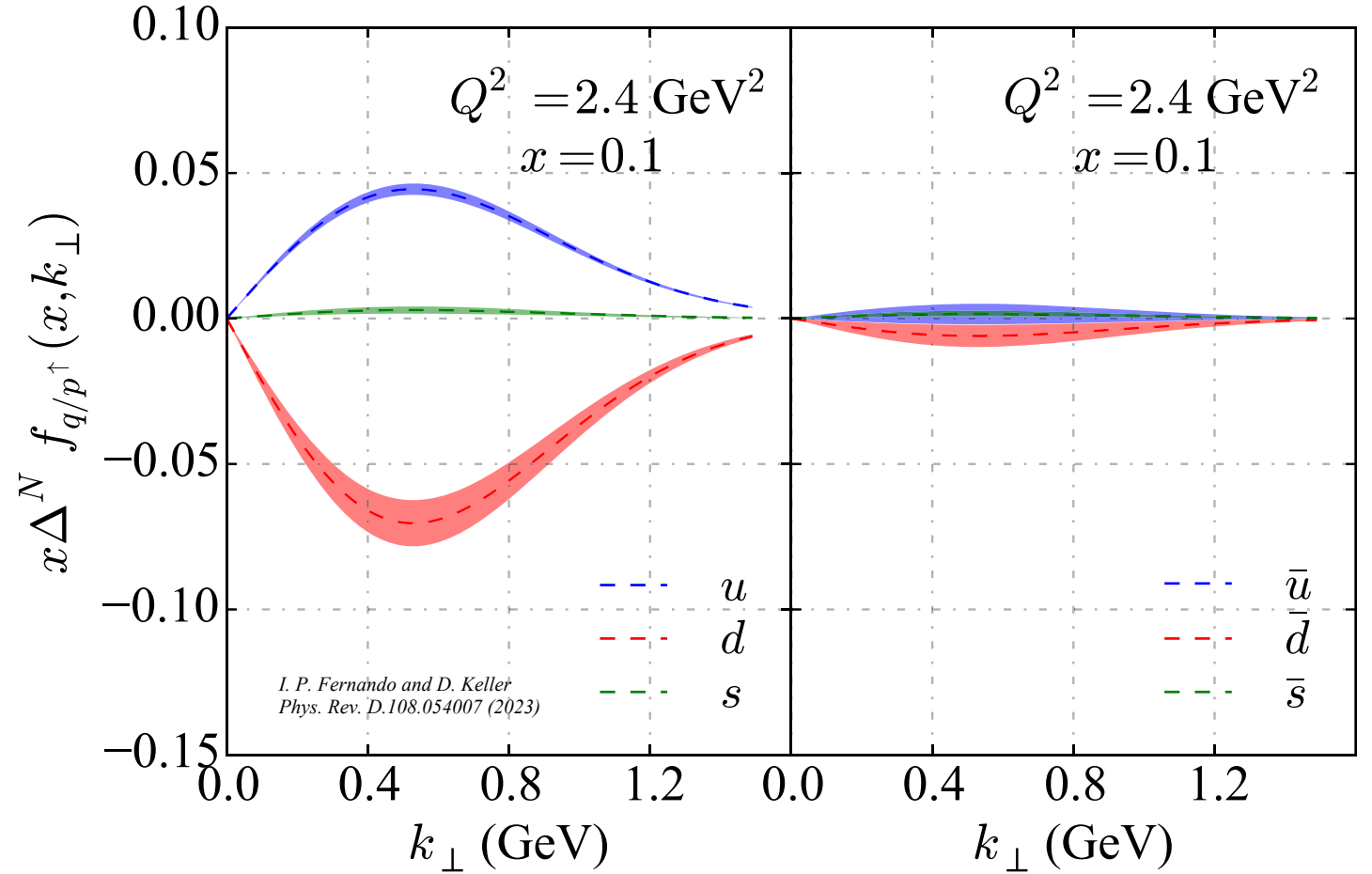


FIG. 18. Sivers functions from a retrained DNN model using the cuts [65] to the data demonstrating that being selective with the data can reduce the error bands of the fit but may also add an unintentional bias.

# Systematic Studies : TMD Evolution

Backup

The solution of the TMD evolution equations

$$\mu^2 \frac{dF(x, b; \mu, \zeta)}{d\mu^2} = \frac{\gamma_F(\mu, \zeta)}{2} F(x, b; \mu, \zeta)$$

$$\zeta \frac{dF(x, b; \mu, \zeta)}{d\zeta} = -\mathcal{D}(b, \mu) F(x, b; \mu, \zeta),$$

$$F(x, b; \mu, \zeta) = \left( \frac{\zeta}{\zeta_\mu(b)} \right)^{-\mathcal{D}(b, \mu)} F(x, b)$$

$$\mu \sim Q, \quad \zeta_F \zeta_D \sim Q^4, \quad \mu^2 = \zeta^2 = Q^2$$

$$\mathcal{N}_q(x) \longrightarrow \mathcal{N}_q(x, Q^2)$$

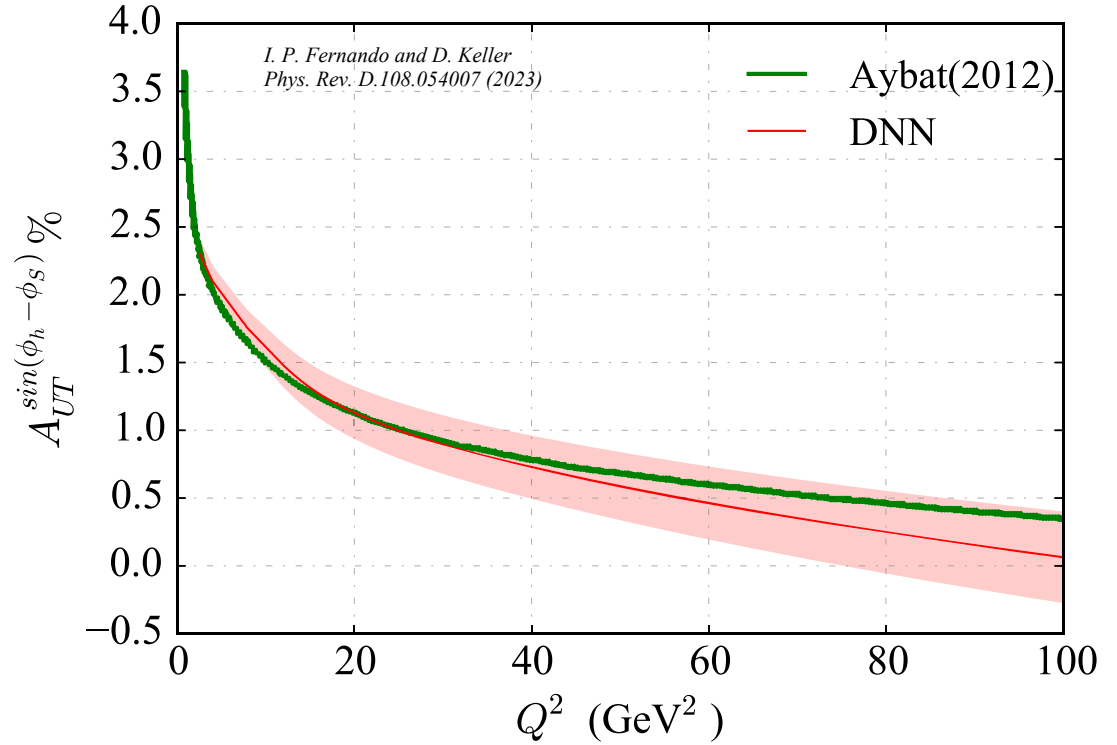


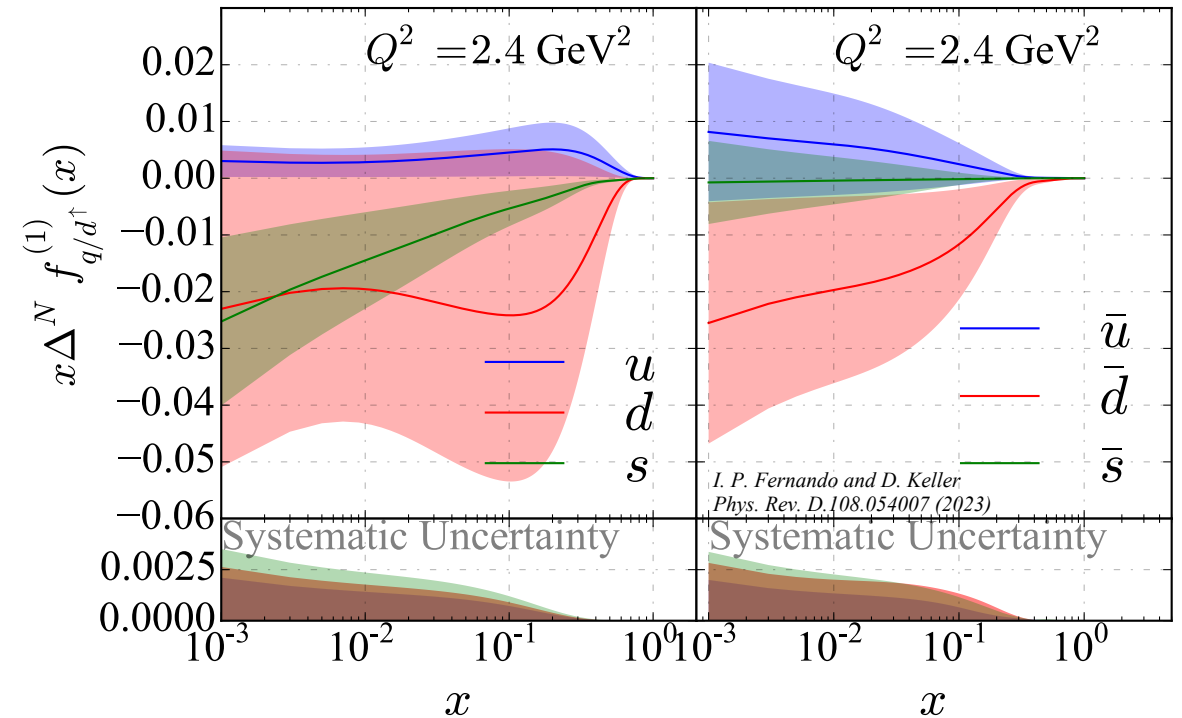
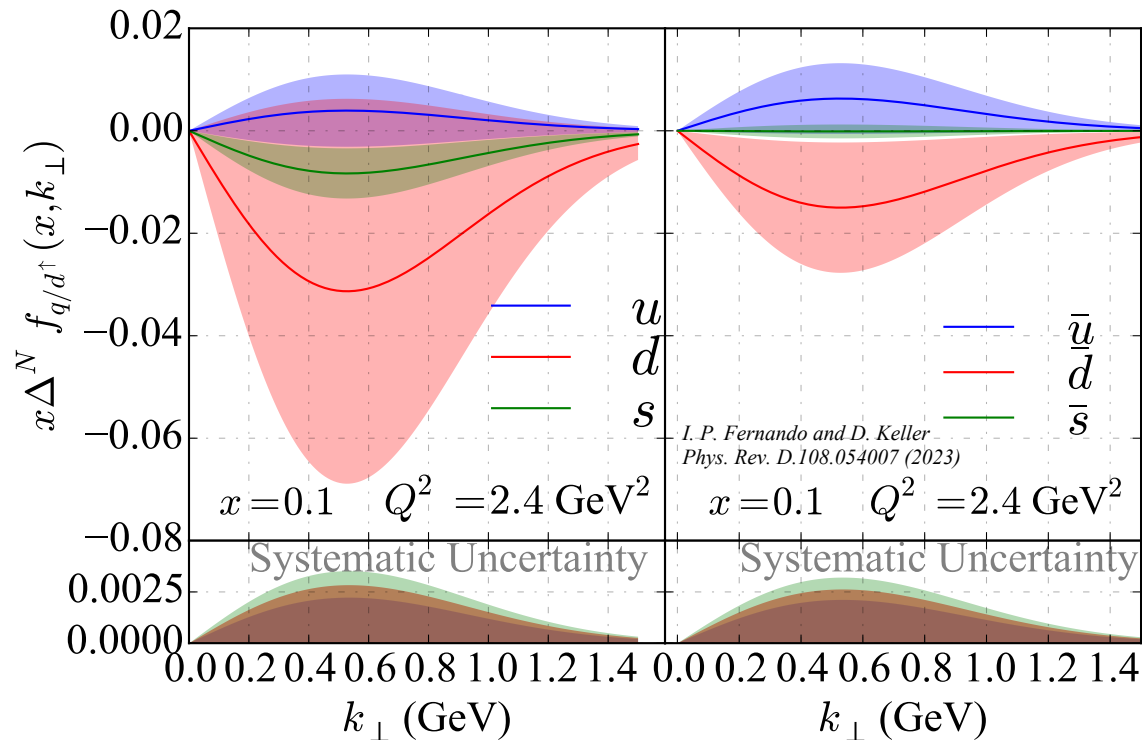
FIG. 21. The Sivers asymmetry evolution in  $Q^2$  compared to the result from [6]. The red-colored solid line and the band represent the mean and standard deviation of the  $A_{UT}^{\sin(\phi_h - \phi_S)}$  from 1000 replica models of the proton DNN at  $x = 0.12$ ,  $z = 0.32$ ,  $p_{hT} = 0.14$  GeV.

# DNN Method: Results from the “Deuteron” Model

- Trained on COMPASS 2009 SIDIS data with Deuteron target.
- Did not imposed iso-spin symmetric conditions, or data cuts.

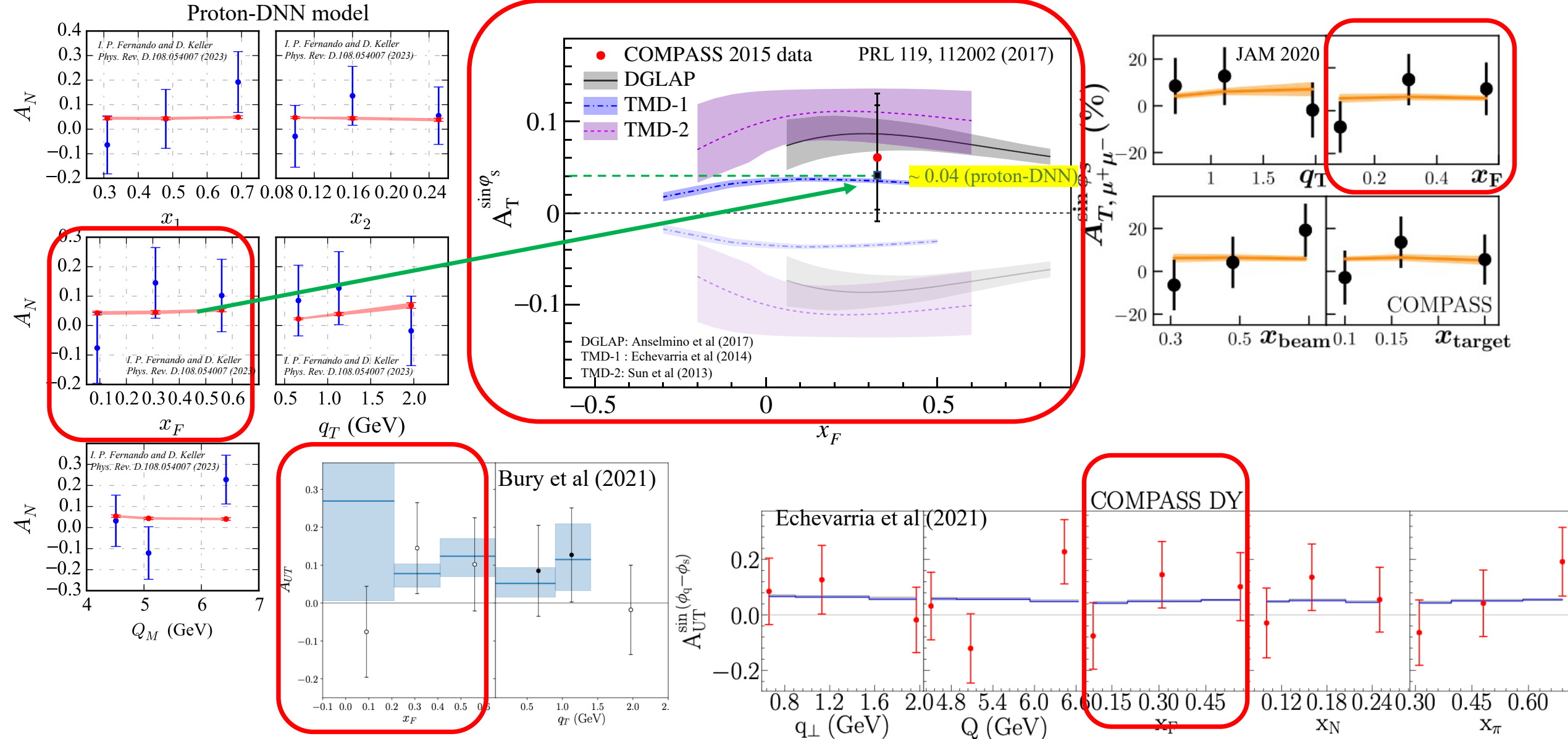
$$\cancel{f_{1T,u\leftarrow d}^\perp = f_{1T,d\leftarrow d}^\perp = \frac{f_{1T,u\leftarrow p}^\perp + f_{1T,d\leftarrow p}^\perp}{2}}$$

$$\Delta^N f_{q/p^\uparrow}^{(1)}(x) = \int d^2 k_\perp \frac{k_\perp}{4m_p} \Delta^N f_{q/p^\uparrow}(x, k_\perp) = -f_{1T}^{\perp(1)q}(x)$$



# DNN Model Projections: DY

COMPASS 2017 DY Projections



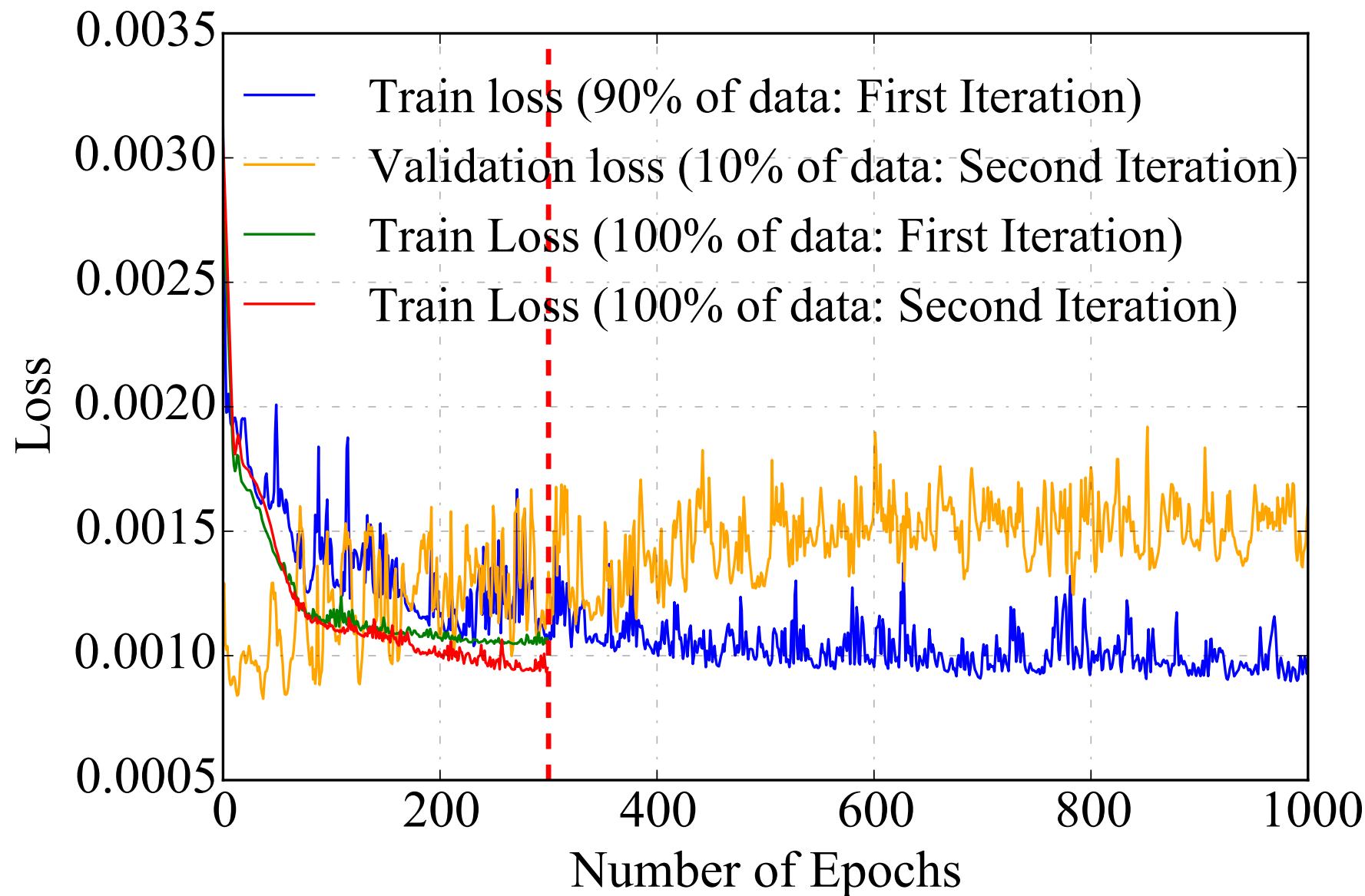


TABLE III. The summary of the optimized sets of hyperparameters: The indications in the table are  $\mathcal{C}_0^i$  and  $\mathcal{C}_0^f$  for results from the pseudodata from the generating function,  $\mathcal{C}_p^i$ , and  $\mathcal{C}_p^f$  for results from SIDIS data from experiments associated with the polarized-proton target, and  $\mathcal{C}_d^i$  and  $\mathcal{C}_d^f$  for results from SIDIS data from experiments associated with the polarized-deuterium target, where  $i$  and  $f$  indicate the *First Iteration* and *Second Iteration* respectively. The initial learning rate is also listed ( $\times 10^{-4}$ ) as is the final training loss ( $\times 10^{-3}$ ). The accuracy and precision in each case are the maxima over the phase space.

Hyperparameter	$\mathcal{C}_0^i$	$\mathcal{C}_0^f$	$\mathcal{C}_p^i$	$\mathcal{C}_p^f$	$\mathcal{C}_d^i$	$\mathcal{C}_d^f$
Hidden layers	5	7	5	7	5	8
Nodes/layer	256	256	550	550	256	256
Learning rate	1	0.125	5	1	10	1
Batch size	200	256	300	300	100	20
Number of epochs	1000	1000	300	300	200	200
Training loss	0.6	0.05	1.5	1	2	1
$\epsilon_u^{\max}$	95.67	99.27	55.21	94.04	56.80	93.02
$\epsilon_{\bar{u}}^{\max}$	42.62	98.09	52.57	96.70	34.83	91.40
$\epsilon_d^{\max}$	80.46	98.89	55.69	93.13	52.44	89.27
$\epsilon_{\bar{d}}^{\max}$	74.59	97.08	55.37	95.04	46.60	92.58
$\epsilon_s^{\max}$	45.53	79.27	49.54	90.64	36.34	93.41
$\epsilon_{\bar{s}}^{\max}$	59.27	91.13	33.89	82.51	65.57	91.45
$\sigma_u^{\max}$	3	0.1	5	2	2	0.4
$\sigma_{\bar{u}}^{\max}$	2	0.2	6	2	8	2
$\sigma_d^{\max}$	10	1	20	6	2	1
$\sigma_{\bar{d}}^{\max}$	7	4	20	8	7	1
$\sigma_s^{\max}$	2	0.2	4	1	6	2
$\sigma_{\bar{s}}^{\max}$	1	0.1	4	2	6	3